bioRxiv preprint doi: https://doi.org/10.1101/601377; this version posted May 17, 2019. The copyright holder for this preprint (which was not certified by peer review) is the author/funder, who has granted bioRxiv a license to display the preprint in perpetuity. It is made available under aCC-BY 4.0 International license.

Is amphistomy an adaptation to high light? Optimality models of stomatal traits along light gradients

Christopher D. Muir[1]

[1] Department of Botany, University of Hawai'i, Honolulu, Hawai'i 96822, USA
cdmuir@hawaii.edu
+1 (808) 956-6704
3190 Maile Way
Room 101
Honolulu, HI 96822

Abstract

Stomata regulate the supply of CO_2 for photosynthesis and the rate of water loss out of the leaf. The presence of stomata on both leaf surfaces, termed amphistomy, increases photosynthetic rate, is common in plants from high light habitats, and rare otherwise. In this study I use optimality models based on leaf energy budget and photosynthetic models to ask why amphistomy is common in high light habitats. I developed an R package **leafoptimizer** to solve for stomatal traits that optimally balance carbon gain with water loss in a given environment. The model predicts that amphistomy is common in high light because its marginal effect on carbon gain is greater than in the shade, but only if the costs of amphistomy are also lower under high light than in the shade. More generally, covariation between costs and benefits may explain why stomatal and other traits form discrete phenotypic clusters.

Keywords

adaptation, amphistomatous, energy balance, hypostomatous, leaf temperature, light, optimality, photosynthesis, stomata, stomatal conductance, stomatal ratio

Introduction

Stomata are microscopic pores formed by a pair of guard cells primarily located on the leaf surface of land plants. Their density and aperture on a leaf control the CO_2 supply to leaf interiors and the rate of water lost through transpiration (recently reviewed in Sack & Buckley, 2016). Higher densities and/or larger pores allow more CO_2 into the leaf, increasing photosynthetic rate, but also increasing transpiration (Farquhar & Sharkey, 1982). As the balance of CO_2 and water demand

bioRxiv preprint doi: https://doi.org/10.1101/601377; this version posted May 17, 2019. The copyright holder for this preprint (which was not certified by peer review) is the author/funder, who has granted bioRxiv a license to display the preprint in perpetuity. It is made available under aCC-BY 4.0 International license.

and supply shifts through time and space, stomata respond over minutes to daily environmental variation, throughout the life of a single plant, and over long periods of evolutionary time (Wolfe, 1971; Woodward, 1987; Royer, 2001; Beerling & Royer, 2011; Milla *et al.*, 2013; McElwain & Steinthorsdottir, 2017).

A less appreciated aspect of stomata is that most leaves have all their stomata on the lower (usually abaxial) surface of the leaf, termed hypostomy, while some have them on both surfaces, termed amphistomy (Metcalfe & Chalk, 1950; Peat & Fitter, 1994; Muir, 2015; Drake *et al.*, 2019). Although amphistomy is rare in general, it is common among high light plants (Salisbury, 1927; Mott *et al.*, 1984; Peat & Fitter, 1994; Bucher *et al.*, 2017; Jordan *et al.*, 2014; Muir, 2018; Drake *et al.*, 2019). Why is amphistomy common in high light habitats but rare elsewhere? Amphistomy creates a second parallel pathway for CO_2 diffusion into the leaf, which should increase photosynthesis especially when there is a lot of resistance to diffusion in the mesophyll (Parkhurst, 1978; Gutschick, 1984; Jones, 1985; Parkhurst & Mott, 1990). We might then expect amphistomy to be common, but it is not, implying some cost of amphistomy. Amphistomy also increases transpiration by forming a second boundary layer conductance for water transport (Foster & Smith, 1986, this study), but it is not clear if this tradeoff, or some other, explains variation in stomatal ratio. To evaluate these hypotheses and generate testable predictions, we need theory to predict how trait optima change across environments, both plastically and adaptively. These are classic evolutionary questions.

Stomata are also a fascinating and useful system for understanding phenotypic evolution. Land plants, like all major groups, can thrive in vastly different niches because of their diverse forms and functions, adaptations that evolved over millions of years. Less appreciated, but equally important in the study of phenotypic evolution, is that organisms occupy a small fraction of the feasible phenotypic space that could evolve in principle. This is true of stomata, as I will explain below. Why do some trait values rarely or never evolve? Three broad hypotheses explain why certain phenotypes can be rare or even absent from nature: 1) **Developmental inaccessibility** - a trait value is physically possible and would be favored by selection, but cannot evolve because the developmental system prevents the right genetic variation from arising; 2) **Rare environments** - a trait value is physically possible and would be favored by selection, but is rare because the environment that favors it is itself rare; and 3) **Selection** - a trait value is physically possible but is universally less fit than other trait values. Often, these hypotheses might be referred to as different phenotypic constraints (Arnold, 1992), but this terminology can be fraught with confusion and competing interpretations. In this paper, I focus on evaluating hypothesis 3, but address others throughout. Developmental inaccessibility could be important if mutations that initiate stomatal development on the upper leaf surface cause it to have the same stomatal density and size as the lower surface. This would make it easy to evolve amphistomy from hypostomy, but difficult to evolve different stomatal densities on each surface. It is also not hard to imagine that if there are discrete niches in the environment, then trait values should cluster around values best suited to those niches (Fig. 1D-F). It is more difficult to explain why trait values would cluster when the underlying environment is continuous because this implies that intermediate phenotypes are not favored in intermediate environments (Fig. 1G-I). This pattern would imply a nonlinear relationship between trait optima and environmental gradients.

The ratio of stomatal densities on the upper surface to the sum of both surfaces (hereafter termed "stomatal ratio"), is a great system for studying why traits cluster because the distribution of this trait is highly clustered and we have mathematical tools to predict the optimal trait value in different environments. Stomatal ratio forms three main trait clusters in angiosperms (Muir, 2015):

bioRxiv preprint doi: https://doi.org/10.1101/601377; this version posted May 17, 2019. The copyright holder for this preprint (which was not certified by peer review) is the author/funder, who has granted bioRxiv a license to display the preprint in perpetuity. It is made available under aCC-BY 4.0 International license.

hypostomy (stomatal ratio = 0); complete amphistomy (stomatal ratio = 0.5); and hyperstomy (aka epistomy, stomatal ratio = 1). There are relatively few species with intermediate values, though they do exist and there is genetic variation, suggesting that development does not preclude the evolution of intermediate trait value (Muir *et al.*, 2014a,b, 2015). Few plants (mostly aquatic) are hyperstomatous (epistomatous), so I focus on the "bimodal" pattern describing two clusters, hypo- and amphistomy. Intermediate environments that favor intermediate stomatal ratios might be rare (Fig. 1D-F) or there may be a threshold-like relationship between the environment the trait optimum (Fig. 1H). To evaluate these hypotheses requires predictions about the relationship between the environment and trait optima.

Optimality models provide an independent way to predict the relationship between environments and trait optima against which we can compare observations of the natural world. They are an important part of identifying adaptive variation because "concordance between [optimality] model[s] and nature suggests adaptation" (Olson & Arroyo-Santos, 2015). Optimality models have a long history in successfully explaining plant form and function (Givnish, 1986, 1987), especially with stomata (Cowan & Farquhar, 1977; Buckley *et al.*, 2017b). Optimality models based on physics and chemistry are combined with a "goal" function to generate testable predictions about how traits *should* vary if organisms are adapted to their environment. If optimality models predict phenotypes that do not exist in nature, this might suggest developmental inaccessibility or rare environments prevent the phenotype from evolving. Optimality models may also fail if the "goal" function, assuming it is anything other than fitness, is misspecified.

In this study, I use optimality models to predict stomatal conductance and stomatal ratio across light gradients to evaluate under what conditions, if any, we would expect phenotypic clustering to evolve along a continuous environmental gradient (hypothesis 3). I also evaluate models on their ability to predict other, independent empirical observations. Ideally, a single model should account for all of the following observations: 1) amphistomy is rare (Metcalfe & Chalk, 1950; Peat & Fitter, 1994; Muir, 2015; Drake *et al.*, 2019); 2) amphistomy is more common in high light environments (Salisbury, 1927; Mott *et al.*, 1984; Mott & Michaelson, 1991; Peat & Fitter, 1994; Jordan *et al.*, 2014; Bucher *et al.*, 2017; Muir, 2018; Drake *et al.*, 2019); 3) amphistomy is associated with higher stomatal density (Beerling & Kelly, 1996; Muir, 2018), which is often a proxy for operational stomatal conductance (Franks & Beerling, 2009); and 4) stomatal ratio is bimodal (see above). Amphistomy is also more common in herbs than woody plants (Muir (2015, 2018), but see Drake *et al.* (2019)), but I do not address this observation here.

I examine three models with increasing complexity (Models 1–3). Model 1 assumes no extrinsic "cost" of amphistomy. It asks simply whether a tradeoff between carbon gain and water loss can explain the aforementioned empirical observations. Model 2 adds an extrinsic, *ad hoc* cost of amphistomy but is agnostic about the mechanism underlying this cost (see Discussion). Finally, Model 3 assumes that the extrinsic cost of amphistomy is not constant, but covaries with light gradients.

Materials and Methods

I used biophysical and biochemical models of leaf temperature and photosynthesis to solve for the optimal stomatal conductance and stomatal ratio across different environments. The details of the leaf temperature and photosynthetic models are described elsewhere (Muir, 2019a,b), so I briefly summarize their structure here. A glossary of model inputs and outputs can be found in Tables 1

bioRxiv preprint doi: https://doi.org/10.1101/601377; this version posted May 17, 2019. The copyright holder for this preprint (which was not certified by peer review) is the author/funder, who has granted bioRxiv a license to display the preprint in perpetuity. It is made available under aCC-BY 4.0 International license.

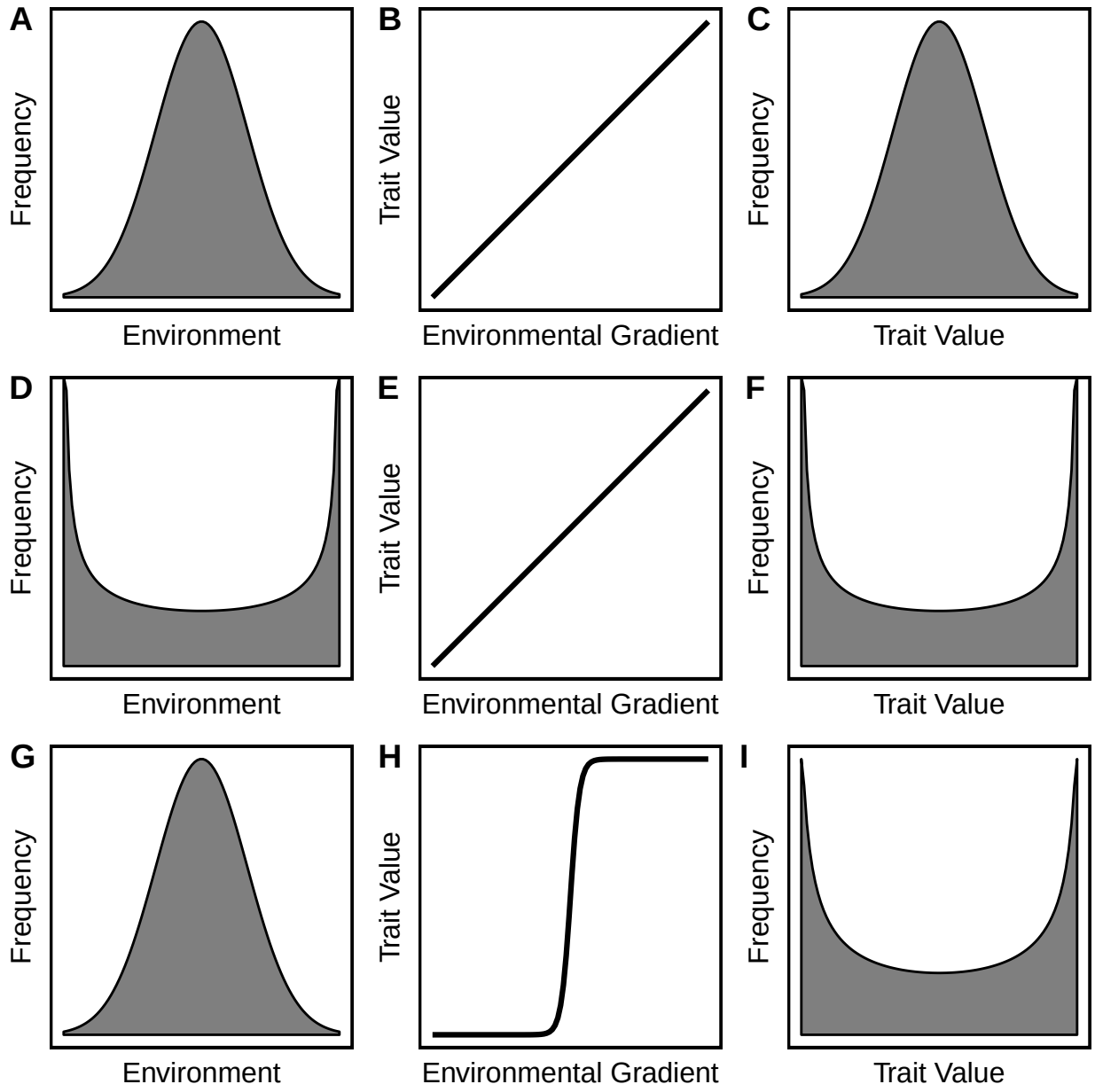

Figure 1: General hypotheses for clustering: No clustering occurs when the environment is unimodal and there is one-to-one matching between the environment and trait optima, leading to a unimodal trait distribution (top row, **A-C**). Clustering can occur if the environment is bimodal even with one-to-one matching between the environment and trait optima (middle row, **D-F**). Clustering can also occur if the environment is unimodal, but there is a nonlinear relationship between the environment and the trait optimum (bottom row, **G-I**). These latter two hypotheses are not mutually exclusive and may reinforce or counteract one another.

and 2, respectively. Values of photosynthetic temperature response functions and fixed parameters are described in Tables S1 and S2 – S4, respectively.

bioRxiv preprint doi: https://doi.org/10.1101/601377; this version posted May 17, 2019. The copyright holder for this preprint (which was not certified by peer review) is the author/funder, who has granted bioRxiv a license to display the preprint in perpetuity. It is made available under aCC-BY 4.0 International license.

Leaf temperature model

I modeled equilibrium leaf temperature using energy budget models (recently reviewed in Gutschick, 2016) implemented using the R package **tealeaves** version 1.0.1 (Muir, 2019b). Given a set of leaf parameters, environmental parameters, and physical constants, leaf energy budget models find the leaf temperature (T_{leaf}) such that the net energy flux in W m^{-2} is balanced:

$$R_{\mathrm{abs}} = S_{\mathrm{r}} + H + L \tag{1}$$

where R_{abs} is the absorbed radiation, S_{r} is infrared re-radiation, H is sensible heat loss, and L is latent heat loss. Absorbed radiation and infrared re-radiation are largely determined by the environment and not affected by stomatal traits. Leaf traits, especially leaf size, strongly impact sensible heat flux (H), but stomatal traits do not affect these properties directly. Stomatal traits strongly affect the total conductance to water vapor (g_{tw}), which is proportional to the latent heat lost (L) as liquid water vaporizes and exits the leaf as a gas:

$$L = h_{\mathrm{vap}} g_{\mathrm{tw}} d_{\mathrm{wv}} \tag{2}$$

tealeaves models the latent heat of vaporization (h_{vap}) as a linear function of temperature (Muir, 2019b; Nobel, 2009). d_{wv} is the water vapor pressure differential from the inside to the outside of leaf in units of mol m^{-3}:

$$d_{\mathrm{wv}} = p_{\mathrm{leaf}}/(\bar{R}T_{\mathrm{leaf}}) - RHp_{\mathrm{air}}/(\bar{R}T_{\mathrm{air}}) \tag{3}$$

I assume the leaf interior is fully saturated (p_{leaf} is the saturation water vapor pressure at T_{leaf}), where the saturation water vapor pressure is a function of temperature calculated using the Goff-Gratch equation (Vömdel, 2016). The vapor pressure of air is the product of the relative humidity (RH) and p_{air}, the saturation water vapor pressure T_{air}.

g_{tw} is the sum of the parallel lower (usually abaxial) and upper (usually adaxial) conductances in units of m s^{-1}, which is the convention in leaf energy budget models:

$$g_{\mathrm{tw}} = g_{\mathrm{w,lower}} + g_{\mathrm{w,upper}} \tag{4}$$

The conductance to water vapor on each surface (indexed as j) is a function of parallel stomatal ($g_{\mathrm{sw},j}$) and cuticular ($g_{\mathrm{uw},j}$) conductances in series with the boundary layer conductance ($g_{\mathrm{bw},j}$). The stomatal and cuticular conductances on the lower surface are:

$$g_{\mathrm{sw,lower}} = [g_{\mathrm{sw}}(1 - SR)][\bar{R}(T_{\mathrm{leaf}} + T_{\mathrm{air}})/2] \tag{5}$$
$$g_{\mathrm{uw,lower}} = (g_{\mathrm{uw}}/2)[\bar{R}(T_{\mathrm{leaf}} + T_{\mathrm{air}})/2] \tag{6}$$

Note that the *total* leaf stomatal and cuticular conductances (g_{sw} and g_{uw} respectively) are in units of μmol H_2O m^{-2} s^{-1} Pa^{-1} in keeping with conventions of photosynthetic models (see below). In the above equations, these values are converted to units of m s^{-1} using the ideal gas law for the leaf energy budget model. Stomatal conductance is partitioned among leaf surfaces depending on

bioRxiv preprint doi: https://doi.org/10.1101/601377; this version posted May 17, 2019. The copyright holder for this preprint (which was not certified by peer review) is the author/funder, who has granted bioRxiv a license to display the preprint in perpetuity. It is made available under aCC-BY 4.0 International license.

stomatal ratio (SR). When $SR = 0$, all conductance is on the lower surface; when $SR = 1$, all conductance is on the upper surface; when $SR = 0.5$, conductance is evenly divided across surfaces. Cuticular conductance is assumed equal on each leaf surface, though this is probably not true in nature (Karbulková *et al.*, 2008). The corresponding expressions for the upper surface are:

$$g_{\mathrm{sw,upper}} = (g_{\mathrm{sw}} SR)[\bar{R}(T_{\mathrm{leaf}} + T_{\mathrm{air}})/2] \tag{7}$$

$$g_{\mathrm{uw,upper}} = g_{\mathrm{uw,lower}} \tag{8}$$

The boundary layer conductances for each surface differ because free convection differs on each surface (Foster & Smith, 1986):

$$g_{\mathrm{bw},j} = \frac{D_w Sh_j}{d} \tag{9}$$

d is the leaf characteristic dimension in m, a physiologically relevant measure of leaf size because it determines heat and mass transfer (Taylor, 1975; Leigh *et al.*, 2017). D_w is the diffusion coefficient of water vapor in air as a function of temperature in units of $\mathrm{m}^2\ \mathrm{s}^{-1}$:

$$D_w = D_{w,0}\left(\frac{T}{273.15}\right)^{eT} \frac{101.3246}{P} \tag{10}$$

Each surface has its own unitless Sherwood number (Sh) that is a mix of free and forced convection:

$$Sh^{3.5} = Sh_{\mathrm{forced}}^{3.5} + Sh_{\mathrm{free}}^{3.5} \tag{11}$$

$$Sh_{\mathrm{forced}} = Nu_{\mathrm{forced}}(D_h/D_w)^{\frac{1}{3}} \tag{12}$$

$$Sh_{\mathrm{free}} = Nu_{\mathrm{free}}(D_h/D_w)^{\frac{1}{4}} \tag{13}$$

The Nusselt number (Nu) is a dimensionless number for heat transfer (Monteith & Unsworth, 2013). Free convection dominates when the Archimedes number (Ar) is greater than 10; forced convection dominates when $Ar \ll 0.1$ (Nobel, 2009). Forced convection is probably most common in nature (Jones, 2014), but free convection can be important for large leaves at low wind speeds (see Muir, 2019b, for further detail). Because free convection depends on gravity, horizontally oriented leaves will exchange latent heat differently depending on how transpiration through stomata is distributed between surfaces. D_h is the diffusion coefficient of heat in air a function of temperature in units of $\mathrm{m}^2\ \mathrm{s}^{-1}$, calculated following Eqn 10 with $D_{h,0}$ substituted for $D_{w,0}$ (Table 1).

Transpiration rate (mol H_2O $\mathrm{m}^{-2}\ \mathrm{s}^{-1}$) is the product of the total conductance to water vapour (Eqn 4) and the water vapor gradient (Eqn 3):

$$E = g_{\mathrm{tw}} d_{\mathrm{wv}} \tag{14}$$

Foster & Smith (1986) previously demonstrated that amphistomatous leaves transpire more water than hypostomatous leaves at low wind speeds, holding total g_{sw} constant. To illustrate this result, I analyzed a similar model using **tealeaves** for hypostomatous ($SR = 0$), intermediate

bioRxiv preprint doi: https://doi.org/10.1101/601377; this version posted May 17, 2019. The copyright holder for this preprint (which was not certified by peer review) is the author/funder, who has granted bioRxiv a license to display the preprint in perpetuity. It is made available under aCC-BY 4.0 International license.

(SR = 0.25), and amphistomatous (SR = 0.5) leaves. I varied wind speed between 0 and 2 m s^{-1} at two light levels, photosynthetic photon flux density (PPFD) = 500 (shade) and 1500 (sun) μmol quanta m^{-2} s^{-1}. I fixed other leaf parameters as absortivity of shortwave radiation (α_s) = 0.5, absorbtivity of longwave radiation (α_l) = 0.97, d = 0.1 m, g_{sw} = 2 μmol H_2O m^{-2} s^{-1} Pa^{-1}, g_{uw} = 0.1 μmol H_2O m^{-2} s^{-1} Pa^{-1}. I fixed other environmental parameters where: atmospheric pressure (P) = 101.3246 kPa, relative humidity (RH) = 0.5, albedo (r) = 0.2, and air temperature (T_{air}) = 25 °C. Physical constants are described in Table 1. I calculated the ratio of transpiration for an intermediate or amphistomatous leaf (E_j) compared to that of hypotstomatous (E_{hypo}) leaf in the same environment:

$$\frac{E_j}{E_{hypo}} \tag{15}$$

Photosynthesis model

The **photosynthesis** package version 1.0.1 (Muir, 2019a) implements the Farquhar-von Caemmerer-Berry biochemical model of C_3 photosynthesis (Farquhar *et al.*, 1980), which has been reviewed extensively elsewhere (e.g. Sharkey *et al.*, 2007). Following the treatment of Buckley & Diaz-Espejo (2015), the photosynthetic demand rate (A_D) is the minimum of Rubisco-, RuBP regeneration-, and TPU-limited assimilation rates:

$$A_D = (1 - \Gamma^*/C_{chl}) \min(W_{carbox}, W_{regen}, W_{tpu}) - R_d \tag{16}$$

$$W_{carbox} = \frac{V_{cmax} C_{chl}}{C_{chl} + K_m} \tag{17}$$

$$W_{regen} = \frac{J C_{chl}}{4C_{chl} + 8\Gamma^*} \tag{18}$$

$$W_{tpu} = \frac{3V_{tpu} C_{chl}}{C_{chl} - \Gamma^*} \tag{19}$$

K_m is the Michaelis-Menten constant:

$$K_m = K_C(1 + O/K_O) \tag{20}$$

J is a function Photosynthetic photon flux density (PPFD), obtained by solving the equation:

$$0 = \theta_J J^2 - J(J_{max} + \phi_J \text{PPFD}) + J_{max}\phi_J \text{PPFD} \tag{21}$$

The photosynthetic supply rate (A_S) is the product of the total conductance to CO_2 (g_{tc} [μmol CO_2 m^{-2} s^{-1} Pa^{-1}]) and CO_2 drawdown ($C_{air} - C_{chl}$):

$$A_S = g_{tc}(C_{air} - C_{chl}) \tag{22}$$

To facilitate modeling differentiated upper and lower leaf anatomies, **photosynthesis** allows users to partition boundary, cuticular, stomatal, and mesophyll conductances separately to each surface

bioRxiv preprint doi: https://doi.org/10.1101/601377; this version posted May 17, 2019. The copyright holder for this preprint (which was not certified by peer review) is the author/funder, who has granted bioRxiv a license to display the preprint in perpetuity. It is made available under aCC-BY 4.0 International license.

(similar to Jones, 1985). On surface j, there are two parallel conductances, the cuticular conductance ($g_{\mathrm{uc},j}$) and the in-series conductances through mesophyll ($g_{\mathrm{mc},j}$), stomata ($g_{\mathrm{sc},j}$), and boundary layer ($g_{\mathrm{bc},j}$). Following rules for circuits (Nobel, 2009), the total conductance for surface j is:

$$g_{\mathrm{c},j} = g_{\mathrm{uc},j} + (1/(r_{\mathrm{m},j} + r_{\mathrm{sc},j} + r_{\mathrm{bc},j})) \tag{23}$$

To simplify the formula, I substitute resistance for conductance ($r_x = g_x^{-1}$) above. Boundary layer conductances to CO_2 are calculated as described above for water vapor, but accounting for the different diffusivity of CO_2 and water vapor in air (see Supporting Information for detail). The mesophyll (g_{mc}) conductance is partitioned between layers using the following definitions:

$$g_{\mathrm{mc,lower}} = g_{\mathrm{mc}}(1/(1 + k_{\mathrm{mc}})) \tag{24}$$

$$g_{\mathrm{mc,upper}} = g_{\mathrm{mc}}(k_{\mathrm{mc}}/(1 + k_{\mathrm{mc}})) \tag{25}$$

$$g_{\mathrm{mc}} = g_{\mathrm{mc,lower}} + g_{\mathrm{mc,upper}} \tag{26}$$

$$\tag{27}$$

g_{mc} is the total leaf conductance through meosphyll, partitioned to lower or upper leaf portions based on the partitioning factor k_{mc}. The cuticular conductance to CO_2 (g_{uc}) is converted from that for water vapor (g_{uw}, see Eqns 6, 8) as described in the Supporting Information.

I modeled photosynthetic temperature responses following Bernacchi *et al.* (2002) and Buckley & Diaz-Espejo (2015). Values of temperature-dependent parameters are provided at 25 °C as input (Table 1) and computed at T_{leaf} (Table 2) to determine the photosynthetic rate. The photosynthetic rate A at a given T_{leaf} is determined by solving for the C_{chl} that balances photosynthetic supply and demand rates ($A_D = A_S$).

Parkhurst (1978), Gutschick (1984), and Jones (1985) previously demonstrated that amphistomatous leaves should photosynthesize more than hypostomatous leaves holding other factors constant. To illustrate this result, I used the **photosynthesis** package to model photosynthetic rate for hypostomatous ($SR = 0$), intermediate ($SR = 0.25$), and amphistomatous ($SR = 0.5$) leaves. I varied T_{leaf} between 5 and 40 °C at two levels of g_{sw}, 1 (low) and 4 (high) μmol H_2O m^{-2} s^{-1} Pa^{-1}. I fixed other leaf parameters as $g_{\mathrm{mc},25} = 3$ μmol CO_2 m^{-2} s^{-1} Pa^{-1}, $g_{\mathrm{uc}} = 0.1$ μmol CO_2 m^{-2} s^{-1} Pa^{-1}, $d = 0.1$ m, $J_{\mathrm{max},25} = 150$ μmol CO_2 m^{-2} s^{-1}, $\phi_J = 0.331$, $R_{\mathrm{d},25} = 2$ μmol CO_2 m^{-2} s^{-1}, $\theta_J = 0.825$, $V_{\mathrm{cmax},25} = 100$ μmol CO_2 m^{-2} s^{-1}, $V_{\mathrm{tpu},25} = 200$ μmol CO_2 m^{-2} s^{-1}. I fixed other environmental parameters where: $C_{\mathrm{air}} = 41$ Pa, $O = 21.27565$ kPa, $P = 101.3246$ kPa, PPFD $= 1500$ μmol quanta m^{-2} s^{-1}, $RH = 0.5$, $T_{\mathrm{air}} = T_{\mathrm{leaf}}$, and $u = 2$ m s^{-1}. Physical constants are described in Table 1.

Optimization of stomatal traits

Biophysical and biochemical models like those implemented in **tealeaves** and **photosynthesis** help understand structure-function relationships, but cannot by themselves predict ecological and evolutionary variation. Optimality models with a defined "goal" function make testable predictions about ecological and evolutionary responses to the environment (Givnish, 1986). In plant physiology, optimality models often assume that plants will modify stomatal traits through acclimation (within

bioRxiv preprint doi: https://doi.org/10.1101/601377; this version posted May 17, 2019. The copyright holder for this preprint (which was not certified by peer review) is the author/funder, who has granted bioRxiv a license to display the preprint in perpetuity. It is made available under aCC-BY 4.0 International license.

generations) or adaptation (between generations) to maximize carbon gain minus costs (usually water loss) that have a carbon exchange rate (Cowan & Farquhar, 1977; Buckley *et al.*, 2017b). Assuming a marginal water cost of carbon gain λ_{w} [mol H_2O mol^{-1} CO_2], the total carbon gain rate per area to maximize is:

$$A - E\lambda_{\mathrm{w}}^{-1} \tag{28}$$

This can be thought of as a profit – carbon gain minus water loss multiplied by a water-to-carbon exchange rate – to be maximized. The optimal solution will be where $\partial A/\partial E = \lambda_{\mathrm{w}}^{-1}$. The cost of water increases with the *inverse* of λ_{w}. For consistency in units, E in this equation must be converted from mol to μmol H_2O m^{-2} s^{-1} during optimization. Traditionally, optimization models find the g_{sw} that optimizes carbon gain and water loss, but other traits and other costs can be added for multivariate optimization. Since SR also affects carbon gain and water loss, I jointly find the optimum of both stomatal traits, denoted $g_{\mathrm{sw,opt}}$ and SR_{opt}. I also included an extrinsic cost of upper stomata (λ_{SR} [Pa^{-1}]) in some models (see below):

$$A - E\lambda_{\mathrm{w}}^{-1} - g_{\mathrm{sc,upper}}\lambda_{SR}^{-1} \tag{29}$$

λ_{SR} must have Pa in the denominator so that $g_{\mathrm{sc,upper}}\lambda_{SR}^{-1}$ has units μmol CO_2 m^{-2} s^{-1}. The cost of amphistomy is proportional to the *inverse* of λ_{SR}. When $\lambda_{SR}^{-1} > 0$, this implies that stomatal conductance through the upper surface incurs some additional cost compared to the same conductance through the lower surface (see Discussion). I refer to λ_{SR}^{-1} as an 'extrinsic' cost of amphistomy because it is an *ad hoc* assumption and not an intrinsic part of the mechanistic model. Since the model does not specify mechanistically how this cost arises, I chose values of λ_{SR}^{-1} that yielded nontrivial results, but these values are arbitrary and their realism needs to be tested with experiments.

I developed an R package **leafoptimizer** to integrate leaf energy budget models in **tealeaves** and C_3 photosynthesis models in **photosynthesis** and solve for optimal stomatal traits. **leafoptimizer** takes leaf parameters, environmental parameters, carbon costs, and physical constants as input (Table 1). **leafoptimizer** uses the R package **optimx** (Nash & Varadhan, 2011; Nash, 2014) to numerically solve for the trait optima by iteratively finding 1) the equilibrium T_{leaf} then 2) the E, A, and net carbon balance (Eq. 29) at that T_{leaf} until net carbon balance is maximized. For larger leaves under high light and warm temperatures, $g_{\mathrm{sw,opt}}$ was often unrealistically high to cool leaves down closer to the optimum for photosynthesis (results not shown). Therefore, I set the maximum $g_{\mathrm{sw,opt}}$ to 16.43 μmol H_2O m^{-2} s^{-1} Pa^{-1}, equal to $g_{\mathrm{sc}} = 10$ μmol CO_2 m^{-2} s^{-1} Pa^{-1}). Following Sharkey *et al.* (2007), I use units for conductance that do not change with with atmospheric pressure because they include Pa in the denominator. Often, conductance is reported in units of mol m^{-2} s^{-1} in the physiological literature. When atmospheric pressure is 100 kPa (which is approximately true near sea level), the nominal conductance in pressure-independent units (μmol m^{-2} s^{-1} Pa^{-1}) is 10× greater than the value in units of mol m^{-2} s^{-1}.

$$X\ [\mu\mathrm{mol\ m^{-2}\ s^{-1}\ Pa^{-1}}] \times 100\ [\mathrm{kPa}] \times \frac{10^3\ [\mathrm{Pa}]}{1\ [\mathrm{kPa}]} \times \frac{1\ [\mathrm{mol}]}{10^6\ [\mu\mathrm{mol}]} = 0.1X\ [\mathrm{mol\ m^{-2}\ s^{-1}}]$$

A current version of **leafoptimizer** is available on GitHub (https://github.com/cdmuir/leafoptimizer). The version used for this manuscript (0.0.1) is archived on Zenodo (https://zenodo.org/). I will

bioRxiv preprint doi: https://doi.org/10.1101/601377; this version posted May 17, 2019. The copyright holder for this preprint (which was not certified by peer review) is the author/funder, who has granted bioRxiv a license to display the preprint in perpetuity. It is made available under aCC-BY 4.0 International license.

continue developing the package and depositing revised source code on GitHub between stable release versions. Other scientists can contribute code to improve **leafoptimizer** or modify the source code on their own installations for a more fully customized implementation. A future publication will more fully describe the package and its potential applications. **leafoptimizer** depends on several other R packages: **checkmate** (Lang, 2017), **crayon** (Csárdi, 2017), **dplyr** (Wickham *et al.*, 2018), **glue** (Hester, 2018), **furrr** (Vaughan & Dancho, 2018), **future** (Bengtsson, 2018), **ggplot** (Wickham, 2016), **magrittr** (Bache & Wickham, 2014), **plyr** (Wickham, 2011), **purrr** (Henry & Wickham, 2018a), **rlang** (Henry & Wickham, 2018b), **stringr** (Wickham, 2018), **tibble** (Müller & Wickham, 2019), **tidyr** (Wickham & Henry, 2018), **tidyselect** (Henry & Wickham, 2018c), and **units** (Pebesma *et al.*, 2016).

Model 1: no extrinsic cost of amphistomy

Amphistomy increases E most at low wind speed and in large leaves (Foster & Smith, 1986, this study), conditions most common in forest understories where amphistomy is rare (Salisbury, 1927; Peat & Fitter, 1994; Muir, 2018). Amphistomy also increases A more under high light when CO_2 limits photosynthesis (Jones, 1985; Mott *et al.*, 1984). Therefore, I hypothesized that the increased cost of E and decreased photosynthetic benefit could drive the empirical observation that amphistomy is more common in high light environments (Salisbury, 1927; Mott *et al.*, 1984; Mott & Michaelson, 1991; Peat & Fitter, 1994; Jordan *et al.*, 2014; Bucher *et al.*, 2017; Muir, 2018; Drake *et al.*, 2019). To test whether this hypothesis is plausible, I solved for $g_{\mathrm{sw,opt}}$ and SR_{opt} across a light gradient (PPFD = 100 – 2000) at low (0.2 m s^{-1}) and moderate (2 m s^{-1}) wind speeds for small (d = 0.004 m), medium (d = 0.04 m), and large (d = 0.4 m) leaves. These values were chosen to ensure that free convection would be important at low wind speeds (see Results). The cost of water was $\lambda_{\mathrm{w}}^{-1} = 0.001$ mol CO_2 mol^{-1} H_2O. This value is close to that estimated for forbs and grasses under well-watered conditions (0.000981, Manzoni *et al.* (2011)), which is appropriate here because these functional types vary more in stomatal ratio than woody plants (Muir, 2015, 2018) and this study does not evaluate the effects of drought stress, which would increase $\lambda_{\mathrm{w}}^{-1}$. The extrinsic cost of upper stomata was 0. Other model variables and parameters are described in Table S2. Biochemical parameters at 25 ° C for the photosynthesis model roughly match the average and range of values from global plant surveys (Rogers *et al.*, 2017).

Model 2: extrinsic cost of amphistomy

A fitness cost of upper stomata would explain the rarity of amphistomy in nature (Metcalfe & Chalk, 1979; Peat & Fitter, 1994; Muir, 2015, 2018; Drake *et al.*, 2019). Model 1 tests whether a cost emerges instrinsically as a result of how stomatal ratio affect A and E. In this model, I add an exstrinsic cost to upper stomata by varying $\lambda_{SR}^{-1} = 0.5, 1, 2$ Pa. Higher λ_{SR}^{-1} (lower λ_{SR}) corresponds with a higher cost of conductance through upper stomata. Other parameters were the same or similar to Model 1 (Table S3). Because low versus high biochemical parameters $J_{\mathrm{max,25}}$ and $V_{\mathrm{xmax,25}}$ had little qualitative effect (see Results), I used a single intermediate value for Models 2 and 3.

bioRxiv preprint doi: https://doi.org/10.1101/601377; this version posted May 17, 2019. The copyright holder for this preprint (which was not certified by peer review) is the author/funder, who has granted bioRxiv a license to display the preprint in perpetuity. It is made available under aCC-BY 4.0 International license.

Model 3: extrinsic cost of amphistomy covaries with light

Covariation between fitness costs and benefits can generate threshold-like clines because there is a very narrow window of environments in which intermediate phenotypes are optimal. I tested this by covarying PPFD and λ_{SR}^{-1}, otherwise using the same parameter values as in Model 2 (Table S4). PPFD varied between 73 – 1927. I selected λ_{SR}^{-1} values that weakly, moderately, or strongly covaried with PPFD. λ_{SR}^{-1} varied the least (0.667 – 1.333) under the weak-covariance scenario and the most (0.002 – 1.998) under the strong-covariance scenario. In all cases, I used bivariate Gaussian covariance stucture, but adjusted the range of λ_{SR}^{-1}, as depicted in Fig. S2.

Source code for these simulations is available on GitHub (https://github.com/cdmuir/stomata-light) and archived on Zenodo (https://zenodo.org/).

bioRxiv preprint doi: https://doi.org/10.1101/601377; this version posted May 17, 2019. The copyright holder for this preprint (which was not certified by peer review) is the author/funder, who has granted bioRxiv a license to display the preprint in perpetuity. It is made available under aCC-BY 4.0 International license.

Table 1: Parameter inputs for **leafoptimizer**. Each parameter has a mathematical symbol used in the text, the R character string used in the **leafoptimizer** package, a brief description, and the units. For physical constants, a value is provided where applicable, though users can modify these if desired. Conductances to CO_2 (g_c) are interconvertible with those for water vapour g_w and PPFD is interconvertible with S_{sw} (see Supporting Information).

Symbol	R character	Description	Units
Leaf parameters:			
d	`leafsize`	leaf characteristic dimension	m
α_s	`abs_s`	absorbtivity of shortwave radiation (0.3 - 4 μm)	none
α_l	`abs_l`	absorbtivity of longwave radiation (4 - 80 μm)	none
$g_{mc,25}$	`g_mc25`	mesophyll conductance to CO_2 at 25 °C	μmol CO_2 m^{-2} s^{-1} Pa^{-1}
g_{uc}	`g_uc`	cuticular conductance to CO_2	μmol CO_2 m^{-2} s^{-1} Pa^{-1}
g_{uw}	`g_uw`	cuticular conductance to water vapor	μmol H_2O m^{-2} s^{-1} $Pa^{-1\dagger}$
Γ^*_{25}	`gamma_star25`	chloroplastic CO_2 compensation point at 25 °C	Pa
$J_{max,25}$	`J_max25`	potential electron transport at 25 °C	μmol CO_2 m^{-2} s^{-1}
$K_{C,25}$	`K_C25`	Michaelis constant for carboxylation at 25 °C	Pa
$K_{O,25}$	`K_O25`	Michaelis constant for oxygenation at 25 °C	kPa
k_{mc}	`k_mc`	partition of g_{mc} to lower mesophyll	none
k_{uc}	`k_uc`	partition of g_{uc} to lower surface	none
ϕ_J	`phi_J`	initial slope of the response of J to PPFD	none
$R_{d,25}$	`R_d25`	nonphotorespiratory CO_2 release at 25 °C	μmol CO_2 m^{-2} s^{-1}
θ_J	`theta_J`	curvature factor for light-response curve	none
$V_{cmax,25}$	`V_cmax25`	maximum rate of carboxylation at 25 °C	μmol CO_2 m^{-2} s^{-1}
$V_{tpu,25}$	`V_tpu25`	rate of triose phosphate utilization at 25 °C	μmol CO_2 m^{-2} s^{-1}
Environmental parameters:			
C_{air}	`C_air`	atmospheric CO_2 concentration	Pa
E_q	`E_q`	energy per mole quanta	kJ mol^{-1}
f_{PAR}	`f_par`	fraction of S_{sw} that is photosynthetically active radiation (PAR)	none
O	`O`	atmospheric O_2 concentration	kPa
P	`P`	atmospheric pressure	kPa
PPFD	`PPFD`	photosynthetic photon flux density	μmol quanta m^{-2} s^{-1}
r	`r`	reflectance for short-wave irradiance (albedo)	none
RH	`RH`	relative humidity	none
S_{sw}	`S_sw`	incident short-wave (solar) radiation flux density	W m^{-2}
T_{air}	`T_air`	air temperature	K
u	`wind`	windspeed	m s^{-1}

bioRxiv preprint doi: https://doi.org/10.1101/601377; this version posted May 17, 2019. The copyright holder for this preprint (which was not certified by peer review) is the author/funder, who has granted bioRxiv a license to display the preprint in perpetuity. It is made available under aCC-BY 4.0 International license.

Physical constants:

a, b, c, d	`a, b, c, d`	coefficients for calculating Nu and Sh numbers	none
c_p	`c_p`	heat capacity of air	1.01 J g^{-1} K^{-1}
$D_{c,0}$	`D_c0`	diffusion coefficient for CO_2 in air at 0 °C	12.9×10^{-6} m^2 s^{-1}
$D_{h,0}$	`D_h0`	diffusion coefficient for heat in air at 0 °C	19.0×10^{-6} m^2 s^{-1}
$D_{m,0}$	`D_m0`	diffusion coefficient for momentum in air at 0 °C	13.3×10^{-6} m^2 s^{-1}
$D_{w,0}$	`D_w0`	diffusion coefficient for water vapor in air at 0 °C	21.2×10^{-6} m^2 s^{-1}
ϵ	`epsilon`	ratio of water to air molar masses	0.622
eT	`eT`	exponent for temperature dependence of diffusion	1.75
G	`G`	gravitational acceleration	9.8 m s^{-2}
$\bar{R}$	`R`	ideal gas constant	8.3144598 J mol^{-1} K^{-1}
R_{air}	`R_air`	specific gas constant for dry air	287.058 J kg^{-1} K^{-1}
σ	`s`	Stephan-Boltzmann constant	5.67×10^{-8} W m^{-2} K^{-4}

† conductances are presented in molar units for consistency with literature on photosynthesis but are converted to m s^{-1} using the ideal gas law (see text for details) to match conductance to heat transfer.

Results

Amphistomy increases transpiration and CO_2 assimilation

Output from **tealeaves** and **photosynthesis** packages recapitulate previous work demonstrating that amphistomy increases transpiration (E, Fig. 2A) and photosynthetic CO_2 assimilation (A, Fig. 2B). When free convection is important at low wind speed and/or large leaf size, amphistomatous leaves have up to 1.5 times greater E than a hypostomatous leaf in the same conditions. The difference in E between stomatal ratio phenotypes is less when forced convection prevails at higher wind speeds. Amphistomatous leaves increase photosynthetic rate, all else being equal, by providing an additional parallel pathway for CO_2 diffusion. Interestingly, leaves with intermediate phenotypes (stomatal ratio $[SR] = 0.25$) increase photosynthetic rate nearly as much as completely amphistomatous leaves ($SR = 0.5$, Fig. 2B).

bioRxiv preprint doi: https://doi.org/10.1101/601377; this version posted May 17, 2019. The copyright holder for this preprint (which was not certified by peer review) is the author/funder, who has granted bioRxiv a license to display the preprint in perpetuity. It is made available under aCC-BY 4.0 International license.

Table 2: Calculated parameter outputs for **leafoptimizer**. Each parameter has a mathematical symbol used in the text, the R character string used in the **leafoptimizer** package, a brief description, and the units. Note that $g_{\mathrm{sc,opt}}$ is interconvertible with $g_{\mathrm{sw,opt}}$ and $k_{\mathrm{sc,opt}}$ is interconvertible with SR_{opt} (see Supporting Information).

Symbol	R character	Description	Units
Optimized leaf parameters:			
$g_{\mathrm{sc,opt}}$	`g_sc`	optimal stomatal conductance to CO_2	μmol CO_2 m^{-2} s^{-1} Pa^{-1}
$g_{\mathrm{sw,opt}}$	`g_sw`	optimal stomatal conductance to water vapor	μmol H_2O m^{-2} s^{-1} Pa^{-1}
$k_{\mathrm{sc,opt}}$	`k_sc`	optimal partition of $g_{\mathrm{sc,opt}}$ to lower surface	none
SR_{opt}	`sr`	optimal stomatal ratio	none
Leaf parameters:			
A	`A`	photosynthetic rate	μmol CO_2 m^{-2} s^{-1}
C_{chl}	`C_chl`	chloroplastic CO_2 concentration	Pa
E	`E`	transpiration rate	mol H_2O m^{-2} s^{-1}
g_{h}	`g_h`	boundary layer conductance to heat	m s^{-1}
g_{bc}	`g_bc`	boundary layer conductance to CO_2	μmol CO_2 m^{-2} s^{-1} Pa^{-1}
g_{bw}	`g_bw`	boundary layer conductance to water vapor	μmol H_2O m^{-2} s^{-1} Pa^{-1}
g_{mc}	`g_mc`	mesophyll conductance to CO_2 at T_{leaf}	μmol CO_2 m^{-2} s^{-1} Pa^{-1}
g_{tc}	`g_tc`	total conductance to CO_2	μmol CO_2 m^{-2} s^{-1} Pa^{-1}
g_{tw}	`g_tw`	total conductance to water vapor	μmol H_2O m^{-2} s^{-1} Pa^{-1}
Γ^*	`gamma_star`	chloroplastic CO_2 compensation point at T_{leaf}	Pa
Gr	`Gr`	Grashof number	none
H	`H`	sensible heat flux density	W m^{-2}
J_{max}	`J_max`	potential electron transport at T_{leaf}	μmol CO_2 m^{-2} s^{-1}
K_{C}	`K_C`	Michaelis constant for carboxylation at T_{leaf}	Pa
K_{O}	`K_O`	Michaelis constant for oxygenation at T_{leaf}	kPa
L	`L`	latent heat flux density	W m^{-2}
Nu	`Nu`	Nusselt number	none
R_{abs}	`R_abs`	total absorbed radiation	W m^{-2}
R_{d}	`R_d`	nonphotorespiratory CO_2 release at T_{leaf}	μmol CO_2 m^{-2} s^{-1}
Re	`Re`	Reynolds number	none
Sh	`Sh`	Sherwood number	none
S_{r}	`S_r`	longwave re-radiation	W m^{-2}
T_{leaf}	`T_leaf`	leaf temperature	K
V_{cmax}	`V_cmax`	maximum rate of carboxylation at T_{leaf}	μmol CO_2 m^{-2} s^{-1}
V_{tpu}	`V_tpu`	rate of triose phosphate utilization at T_{leaf}	μmol CO_2 m^{-2} s^{-1}
Temperature-dependent physical parameters:			
D_c	`D_c`	diffusion coefficient for CO_2 in air at T_{leaf}	m^2 s^{-1}
D_h	`D_h`	diffusion coefficient for heat in air at T_{leaf}	m^2 s^{-1}
D_m	`D_m`	diffusion coefficient for momentum in air at T_{leaf}	m^2 s^{-1}
D_w	`D_w`	diffusion coefficient for water vapor in air at T_{leaf}	m^2 s^{-1}

bioRxiv preprint doi: https://doi.org/10.1101/601377; this version posted May 17, 2019. The copyright holder for this preprint (which was not certified by peer review) is the author/funder, who has granted bioRxiv a license to display the preprint in perpetuity. It is made available under aCC-BY 4.0 International license.

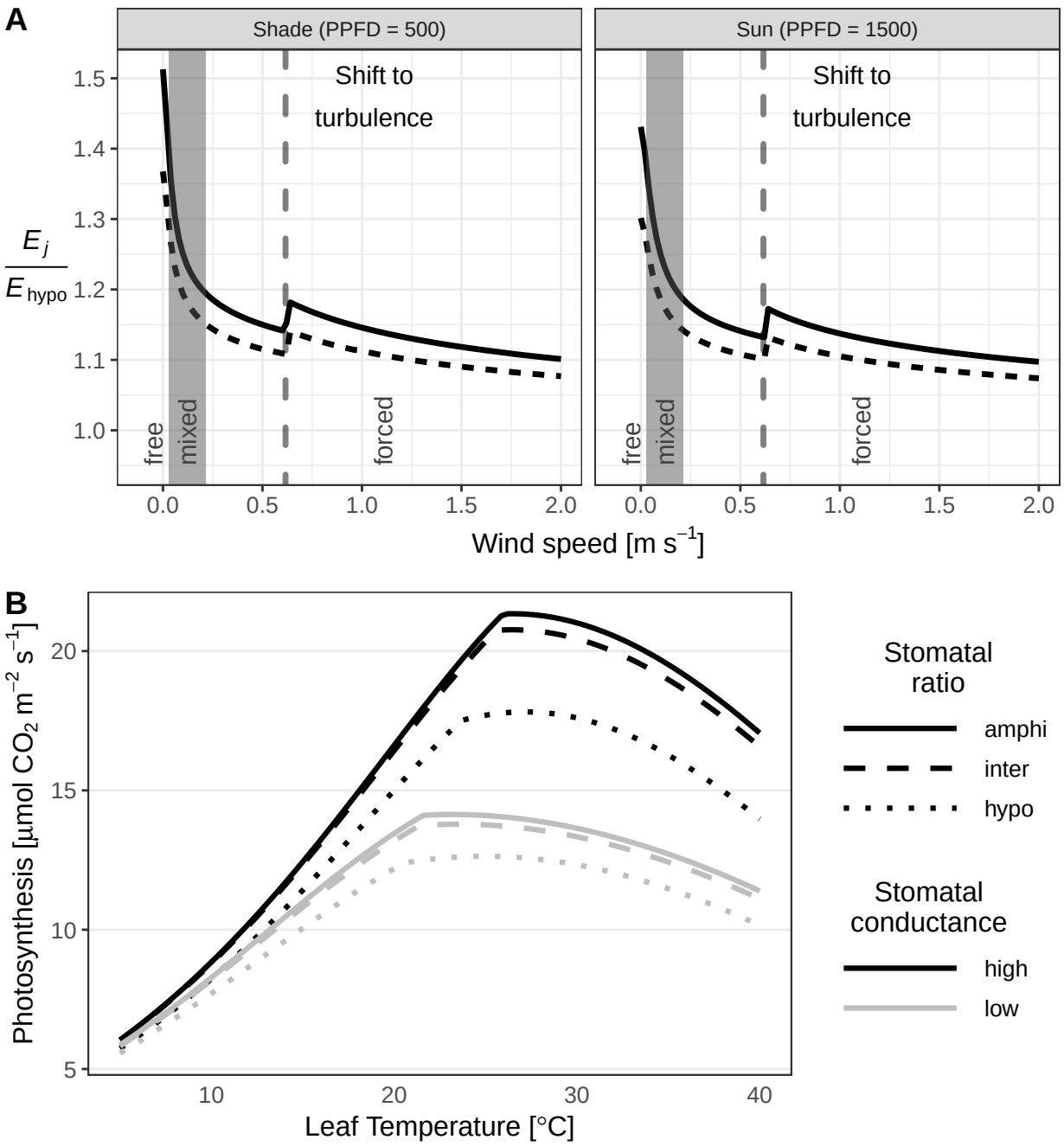

bioRxiv preprint doi: https://doi.org/10.1101/601377; this version posted May 17, 2019. The copyright holder for this preprint (which was not certified by peer review) is the author/funder, who has granted bioRxiv a license to display the preprint in perpetuity. It is made available under aCC-BY 4.0 International license.

Figure 2: Amphistomy increases transpiration and CO_2 assimilation. **A**) Output from **tealeaves** shows that amphistomatous (Stomatal Ratio $(SR) = 0.5$, solid black lines) and intermediate ($SR = 0.25$, dashed black lines) leaves transpire more water than hypostomatous leaves ($E_j/E_{\text{hypo}} > 1$) when stomatal conductance and other leaf/environmental parameters are constant. The effect of SR is especially strong at very low wind speeds (*x*-axis) when free convection is significant (low wind speed, $Ar > 10$); it less important for most leaves in which forced convection (high wind speed, $Ar < 0.1$) and turbulent flow ($Re > 4000$, right of dashed line) dominates heat and mass transfer. The effect is similar in both shade (Photosynthetic photon flux density $(\text{PPFD}) = 500\ \mu\text{mol quanta m}^{-2}\ \text{s}^{-1}$, left facet) and sun ($\text{PPFD} = 1500\ \mu\text{mol quanta m}^{-2}\ \text{s}^{-1}$, right facet), although total transpiration is greater in the sun (results not shown). **B**). Output from **photosynthesis** shows that amphistomatous leaves (solid lines) increase photosynthetic rate compared to intermediate (dashed lines) and hypostomatous (dotted lines) leaves under the same conditions. The values of SR are the same as **A**. Stomatal conductance was set to g_{sw} = 1 (low) and 4 (high) $\mu\text{mol H}_2\text{O m}^{-2}\ \text{s}^{-1}\ \text{Pa}^{-1}$. In all conditions, photosynthetic rate peaks at an intermediate temperature. See Materials and Methods for other parameter values.

Model 1: Amphistomy is almost always favored when there is no cost of upper stomata

In this model, I used **leafoptimizer** to solve for the $g_{\text{sw,opt}}$ and SR_{opt} that optimally balances A and E across a range of environmental conditions (Table S2), given a cost of water, but no extrinsic cost of upper stomata.

In almost all areas of parameter space, the additional A associated with amphistomy outweighs the increased E (Fig. 2). A greater fraction of stomata on the lower surface can be beneficial only when reduced transpiration heats the leaf up closer to the optimum for photosynthesis ($T_{\text{leaf}} \approx 25°\text{C}$) given the temperature response parameters assumed in this study [Fig. 2B, Table S1]). This only occurred at suboptimal air temperatures for large leaves in still air at low to moderate irradiance (Fig. 3). Forced convection dominated heat and mass transfer in smaller leaves or leaves in moving air (Figs. 3, S1). Only with the transition to free convection in large leaves and still air does reducing the conductance on the upper surface dramatically decrease transpiration (Fig. 2A). However, this beneficial effect of having lower stomatal conductance on the upper surface goes away under high irradiance because T_{leaf} rises toward the optimal temperature for photosynthesis. Hence, amphistomy is always favored at high irradiance when there is no extrinsic cost of upper stomata (Fig. 3). Biochemical parameters had little qualitative effect on the results (Fig. S3).

Model 2: an extrinsic cost of amphistomy produces correlations with light

Model 1 demonstrated that without an extrinsic cost, amphistomy is nearly always optimal. However, under the same leaf and environmental parameters as Model 1, an extrinsic cost leads to many situations in which hypostomy or intermediate SR are optimal (Fig. 4A). Under low light, hypostomy is better unless the cost of amphistomy is very low, but under high light, SR_{opt} depends strongly on λ_{SR}^{-1}. When the cost is low, an intermediate SR_{opt} occurs at most light levels; when the cost is high, SR_{opt} is always near 0 (hypostomy). This model also predicts some covariation between SR_{opt} and $g_{\text{sw,opt}}$. At low light, both values are predicted to be low; at high light, both values are

bioRxiv preprint doi: https://doi.org/10.1101/601377; this version posted May 17, 2019. The copyright holder for this preprint (which was not certified by peer review) is the author/funder, who has granted bioRxiv a license to display the preprint in perpetuity. It is made available under aCC-BY 4.0 International license.

higher (Fig. 4).

Model 3: low costs of amphistomy at high light can produce threshold-like clines

Compared to Model 2, covariation between costs of amphistomy and light produced stronger threshold-like clines between light and SR_{opt} (Fig. 5). With strong covariance, complete hypostomy ($SR_{\text{opt}} = 0$) was optimal under low light and high λ_{SR}^{-1}; complete amphistomy ($SR_{\text{opt}} = 0.5$) was optimal under high light and low λ_{SR}^{-1}. The correlation between SR_{opt} and $g_{\text{sw,opt}}$ was similar to Model 2.

Table 3: Which model accodomates empirical observations? The empirical observations are that amphistomy is rare, correlated with light habitat, correlated with stomatal density, and is bimodal. See Introduction for further detail. A '✓' indicates that the model can explain this observation.

	Empirical observations			
Amphistomy is:	Rare	Cor with light	Cor with stomatal density	Bimodal
Model 1: No cost of *SR*				
Model 2: Cost of *SR*	✓	✓	✓	
Model 3: Covarying cost of *SR*	✓	✓	✓	✓

Discussion

I used three optimality models based on the biophysics and biochemistry of leaf temperature and photosynthesis to predict stomatal ratio (SR_{opt}) and conductance ($g_{\text{sw,opt}}$) across light gradients. I draw three substantial conclusions about the evolution of stomatal traits that inform more general questions about phenotypic evolution.

First, a tradeoff between increased photosynthetic CO_2 assimilation (A, 2B) and water loss (E, Fig. 2A) does not explain why amphistomy is rare because the benefits almost always outweigh the costs (Model 1, Table 3). Previous modeling and experiments already demonstrated the physiological effects of amphistomy on A and E (Parkhurst, 1978; Gutschick, 1984; Foster & Smith, 1986; Parkhurst & Mott, 1990; Šantrůček *et al.*, 2019), but these insights have not been combined for optimality modeling. Hypostomy is sometimes optimal at low wind speed, low/partial sun, and suboptimal temperatures (Fig. 3, S1) because decreased E brings T_{leaf} closer to its optimum. However, these restrictive conditions are probably not common in nature; even light wind speeds greater than 1 m s^{-1} would completely eliminate this effect (Fig. 3).

Second, an extrinsic cost of amphistomy (λ_{SR}^{-1}) produces a cline between light and SR_{opt} (Model 2, Fig. 4). Under the same parameters in Model 1, no such cline is predicted. A previous phenomenological model also suggested that the cost of amphistomy is important (Muir, 2015), but could not distinguish between an "intrinsic" (Model 1) and "extrinsic" (Models 2 and 3) cost. The leaf temperature and photosynthesis models in this study indicate that the tradeoff between A and E is not the mechanism explaining stomatal ratio, but future mechanistic models of other processes effected by stomatal ratio (e.g. hydraulic conductance outside the xylem (Buckley *et al.*,

bioRxiv preprint doi: https://doi.org/10.1101/601377; this version posted May 17, 2019. The copyright holder for this preprint (which was not certified by peer review) is the author/funder, who has granted bioRxiv a license to display the preprint in perpetuity. It is made available under aCC-BY 4.0 International license.

2015, 2017a; Drake *et al.*, 2019)) may reveal an 'intrinsic' cost. Model 2 also explains why stomatal ratio and conductance positively covary along light gradients (Muir, 2018). Both SR_{opt} and $g_{\text{sw,opt}}$ are beneficial under high light because the marginal benefit of increased CO_2 supply is greater under high light. I am assuming here that stomatal density is a proxy for operational stomatal conductance (Franks & Beerling, 2009). Generally, stomatal density increases with light up to an intermediate value then decreases slightly (Poorter *et al.*, 2019), consistent with model predictions here (Figs. 4B, 5B). However, in real plants, many other traits change in response to light which are forced to remain constant in the model, so this correspondance between model predictions and experiments may be spurious. Overall, this model indicates that optimizing both density and distribution of stomata on a leaf may help plants fully take advantage of high light and should be considered together in future analyses of light responses.

Third, only when the cost of amphistomy covaries with light does a threshold-like trait-environment relationship emerge (Model 3, Fig. 5). Model 2 explains other empirical observations (Table 3) but fails to explain why intermediate stomatal ratio trait values are rare in nature. Under that model, intermediate values should be common. Only by coupling a benefit of increased A under high light with a low cost of amphistomy in the same environment do we predict discrete clusters of hypo- and amphistomatous leaves (i.e. bimodality). Covariation between costs of amphistomy and light may be the only way in this modeling framework to get phenotypic clusters when the underlying environmental gradient is continuous. I used light as an environmental gradient based on *a priori* hypotheses, but covariation between the cost of amphistomy and another environment or trait could produce qualitatively similar results. For example, amphistomy increases A more in leaves with high resistance to mesophyll CO_2 diffusion (Parkhurst, 1978). Covariation between λ_{SR}^{-1} and that trait could also produce a similar effect, but would not necessarily explain why amphistomy is common in high light environments.

The goals of optimality models are to accomodate existing observations and generate new testable predictions. Model 3 accomodates existing observations, but is complex and therefore important to evaluate with future empirical tests of its predictions. In particular, the model implicates the importance of covariation between costs and benefits of amphistomy. Hypostomy is favored in low light with low costs of amphistomy, but high light only favors amphistomy ($SR_{\text{opt}} = 0.5$) when costs are also low. This is important because some proposed costs probably do not covary with light gradients this way, while others likely do. For example, amphistomy can dehydrate the palisade mesophyll when there is strong evaporative demand (Buckley *et al.*, 2017a; Drake *et al.*, 2019), but this cost should be stronger, not weaker, under high light. Furthermore, when leaves can optimize both SR and g_{sw} simultaneously, amphistomatous leaves have lower $g_{\text{sw,opt}}$ and hence lower evaporative demand than hypostomatous plants holding all else constant (Fig. 4). Amphistomy may also be costly if it increases susceptibility to foliar pathogens that are more likely to land on the upper surface of a horizontally oriented leaf (Gutschick, 1984; McKown *et al.*, 2014). Because many pathogens need a wet leaf microclimate to germinate and grow, a leaf in high light that dries faster is less likely to experience this cost than one in the shade. Hence, if pathogens are the primary cost of amphistomy, then this cost should be higher in shady habitats and lower in sunny habitats, consistent with the assumptions of Model 3. Future work should focus on identifying the abiotic and biotic cost(s) of upper stomata at different light levels under natural conditions. We also need to evaluate how often the distribution of light values is unimodal in nature (hypothesis 2) and the role of developmental constraints on stomatal evolution (hypothesis 1).

There are several important limitations of this study that will need to be addressed in future work. Currently **leafoptimizer** only optimizes stomatal traits while other traits are held constant. But

bioRxiv preprint doi: https://doi.org/10.1101/601377; this version posted May 17, 2019. The copyright holder for this preprint (which was not certified by peer review) is the author/funder, who has granted bioRxiv a license to display the preprint in perpetuity. It is made available under aCC-BY 4.0 International license.

traits such as leaf size, mesophyll conductance, $J_{\mathrm{max}}/V_{\mathrm{cmax}}$ acclimate and evolve too. If all these traits could vary together in the model, different patterns might emerge. For example, high light favors thick leaves to capture more photons and greater investment in photosynthetic biochemistry, traits that make increased CO_2 supply more advantageous. In this case, a greater benefit rather than increased cost might explain why amphistomy is common at high light. Furthermore, this study did not exhaustively explore relevant parameter space. It is possible that further exploration may reveal patterns not identified here. For example, I only used a single set of temperature response functions, even those these vary within and between species (Medlyn *et al.*, 2002; Slot & Winter, 2017). However, this limitation does not qualitatively change the result that amphistomy only significantly affects evaporation, and hence leaf temperature, when leaf size is large, wind speed is almost zero, and there is relatively high sunlight. These conditions are not common in nature. Different temperature response parameters that change optimum leaf temperature would alter the range of air temperatures in which hypostomy would helps keep leaf temperature closer its optimum under restrictive parameter spece. The model also uses bulk leaf properties of temperature and photosynthesis at one time point, ignoring spatial variation within the leaf and temporal variation in the environment, which might yield different predictions (Buckley *et al.*, 2017a; Earles *et al.*, 2019). Finally, carbon gain and water loss are not fitness, which is what natural selection cares about. Future theoretical and empirical studies should integrate plant survivorship and reproduction with stomatal function.

Amphistomy is rare despite the fact that it increases photosynthetic rate. Why? Optimality models show this is not because the increased carbon gain is offset by additional water loss. Instead, an additional cost of amphistomy, yet to be identified, must explain why it is rare. Optimality models also predict that amphistomy is common in high light habitats not just because it increases carbon gain but also because the costs of amphistomy are lower. Covariation between costs and benefits may also explain why stomatal ratio forms discrete phenotypic clusters.

Acknowledgements

I would like to thank Joseph Stinziano and an anonymous reviewer for valuable feedback on this work.

Funding

This work was supported by startup funds from the University of Hawai'i.

References

Arnold SJ. 1992. Constraints on phenotypic evolution. *The American Naturalist*, **140**: S85–S107.

Bache SM , Wickham H. 2014. *magrittr: A Forward-Pipe Operator for R*. R package version 1.5.

Beerling DJ , Kelly CK. 1996. Evolutionary comparative analyses of the relationship between leaf structure and function. *New Phytologist*, **134**: 35–51.

bioRxiv preprint doi: https://doi.org/10.1101/601377; this version posted May 17, 2019. The copyright holder for this preprint (which was not certified by peer review) is the author/funder, who has granted bioRxiv a license to display the preprint in perpetuity. It is made available under aCC-BY 4.0 International license.

Beerling DJ , Royer DL. 2011. Convergent Cenozoic CO_2 history. *Nature Geoscience*, **4**: 418–420.

Bengtsson H. 2018. *future: Unified Parallel and Distributed Processing in R for Everyone*. R package version 1.10.0.

Bernacchi CJ, Portis AR, Nakano H, von Caemmerer S , Long SP. 2002. Temperature response of mesophyll conductance. implications for the determination of rubisco enzyme kinetics and for limitations to photosynthesis *in vivo*. *Plant Physiology*, **130**: 1992—-1998.

Bucher SF, Auerswald K, Grün-Wenzel C, Higgins SI, Jorge JG , Römermann C. 2017. Stomatal traits relate to habitat preferences of herbaceous species in a temperate climate. *Flora*, **229**: 107–115.

Buckley TN , Diaz-Espejo A. 2015. Partitioning changes in photosynthetic rate into contributions from different variables. *Plant, Cell & Environment*, **38**: 1200–1211.

Buckley TN, John GP, Scoffoni C , Sack L. 2015. How does leaf anatomy influence water transport outside the xylem? *Plant Physiology*, **168**: 1616–1635.

Buckley TN, John GP, Scoffoni C , Sack L. 2017a. The sites of evaporation within leaves. *Plant Physiology*, **173**: 1763–1782.

Buckley TN, Sack L , Farquhar GD. 2017b. Optimal plant water economy. *Plant, Cell & Environment*, **40**: 881–896.

Cowan IR , Farquhar GD. 1977. Stomatal function in relation to leaf metabolism and environment. *Symposia of the Society for Experimental Biology*, **31**: 471–505.

Csárdi G. 2017. *crayon: Colored Terminal Output*. R package version 1.3.4.

Drake PL, de Boer HJ, Schymanski SJ , Veneklaas EJ. 2019. Two sides to every leaf: water and CO_2 transport in hypostomatous and amphistomatous leaves. *New Phytologist*.

Earles JM, Buckley TN, Brodersen CR, Busch FA, Cano FJ, Choat B, Evans JR, Farquhar GD, Harwood R, Huynh M *et al*. 2019. Embracing 3D complexity in leaf carbon–water exchange. *Trends in Plant Science*, **24**: 15–24.

Farquhar GD, von Caemmerer Sv , Berry J. 1980. A biochemical model of photosynthetic CO_2 assimilation in leaves of C_3 species. *Planta*, **149**: 78–90.

Farquhar GD , Sharkey TD. 1982. Stomatal conductance and photosynthesis. *Annual review of plant physiology*, **33**: 317–345.

Foster JR , Smith WK. 1986. Influence of stomatal distribution on transpiration in low-wind environments. *Plant, Cell & Environment*, **9**: 751–759.

Franks PJ , Beerling DJ. 2009. Maximum leaf conductance driven by CO_2 effects on stomatal size and density over geologic time. *Proceedings of the National Academy of Sciences*, **106**: 10343–10347.

Givnish TJ (ed.) . 1986. *On the economy of plant form and function*. Cambridge University Press, Cambridge.

bioRxiv preprint doi: https://doi.org/10.1101/601377; this version posted May 17, 2019. The copyright holder for this preprint (which was not certified by peer review) is the author/funder, who has granted bioRxiv a license to display the preprint in perpetuity. It is made available under aCC-BY 4.0 International license.

Givnish TJ. 1987. Comparative studies of leaf form: assessing the relative roles of selective pressures and phylogenetic constraints. *New Phytologist*, **106**: 131–160.

Gutschick VP. 1984. Photosynthesis model for C_3 leaves incorporating CO_2 transport, propagation of radiation, and biochemistry 2. ecological and agricultural utility. *Photosynthetica*, **18**: 569–595.

Gutschick VP. 2016. *Leaf Energy Balance: Basics, and Modeling from Leaves to Canopies*, Springer Netherlands, Dordrecht, pp. 23–58.

Henry L , Wickham H. 2018a. *purrr: Functional Programming Tools*. R package version 0.2.5.

Henry L , Wickham H. 2018b. *rlang: Functions for Base Types and Core R and 'Tidyverse' Features*. R package version 0.3.0.1.

Henry L , Wickham H. 2018c. *tidyselect: Select from a Set of Strings*. R package version 0.2.5.

Hester J. 2018. *glue: Interpreted String Literals*. R package version 1.3.0.

Jones HG. 1985. Adaptive significance of leaf development and structural responses to environment. In: *Control of Leaf Growth* (eds. Baker NR., Davies W. & Ong CK.). Cambridge University Press, Cambridge, vol. 27 of *Society for Experimental Biology Seminar Series*, pp. 155–173.

Jones HG. 2014. Plants and microclimate.

Jordan GJ, Carpenter RJ , Brodribb TJ. 2014. Using fossil leaves as evidence for open vegetation. *Palaeogeography, Palaeoclimatology, Palaeoecology*, **395**: 168–175.

Karbulková J, Schreiber L, Macek P , Šantrůček J. 2008. Differences between water permeability of astomatous and stomatous cuticular membranes: effects of air humidity in two species of contrasting drought-resistance strategy. *Journal of Experimental Botany*, **59**: 3987–3995.

Lang M. 2017. checkmate: Fast argument checks for defensive r programming. *The R Journal*, **9**: 437–445.

Leigh A, Sevanto S, Close J , Nicotra A. 2017. The influence of leaf size and shape on leaf thermal dynamics: does theory hold up under natural conditions? *Plant, Cell & Environment*, **40**: 237–248.

Manzoni S, Vico G, Katul G, Fay PA, Polley W, Palmroth S , Porporato A. 2011. Optimizing stomatal conductance for maximum carbon gain under water stress: a meta-analysis across plant functional types and climates. *Functional Ecology*, **25**: 456–467.

McElwain JC , Steinthorsdottir M. 2017. Paleoecology, ploidy, paleoatmospheric composition, and developmental biology: a review of the multiple uses of fossil stomata. *Plant Physiology*, **174**: 650–664.

McKown AD, Guy RD, Quamme L, Klápště J, La Mantia J, Constabel C, El-Kassaby YA, Hamelin RC, Zifkin M , Azam M. 2014. Association genetics, geography and ecophysiology link stomatal patterning in *Populus trichocarpa* with carbon gain and disease resistance trade-offs. *Molecular Ecology*, **23**: 5771–5790.

bioRxiv preprint doi: https://doi.org/10.1101/601377; this version posted May 17, 2019. The copyright holder for this preprint (which was not certified by peer review) is the author/funder, who has granted bioRxiv a license to display the preprint in perpetuity. It is made available under aCC-BY 4.0 International license.

Medlyn B, Dreyer E, Ellsworth D, Forstreuter M, Harley P, Kirschbaum M, Le Roux X, Montpied P, Strassemeyer J, Walcroft A *et al.* 2002. Temperature response of parameters of a biochemically based model of photosynthesis. ii. a review of experimental data. *Plant, Cell & Environment*, **25**: 1167–1179.

Metcalfe CR , Chalk L. 1950. *Anatomy of the dicotyledons, Vols. 1 & 2.* 1st edn. Oxford University Press, Oxford.

Metcalfe CR , Chalk L. 1979. *Anatomy of the dicotyledons, Vols. 1 & 2.* 2nd edn. Clarendon Press, Oxford.

Milla R, de Diego-Vico N , Martín-Robles N. 2013. Shifts in stomatal traits following the domestication of plant species. *Journal of Experimental Botany*, **64**: 3137–3146.

Monteith JL , Unsworth MH. 2013. *Principles of Environmental Physics.* 4th edn. Academic Press.

Mott KA, Gibson AC , O'Leary JW. 1984. The adaptive significance of amphistomatic leaves. *Plant, Cell & Environment*, **5**: 455–460.

Mott KA , Michaelson O. 1991. Amphistomy as an adaptation to high light intensity in *Ambrosia cordifolia* (Compositae). *American Journal of Botany*, **78**: 76–79.

Muir CD. 2015. Making pore choices: repeated regime shifts in stomatal ratio. *Proc. R. Soc. B*, **282**: 20151498.

Muir CD. 2018. Light and growth form interact to shape stomatal ratio among British angiosperms. *New Phytologist*, **218**: 242–252.

Muir CD. 2019a. *photosynthesis: model C3 photosynthesis.* R package version 1.0.1.

Muir CD. 2019b. tealeaves: an r package for modelling leaf temperature using energy budgets. *bioRxiv.*

Muir CD, Conesa MÁ, Roldán E, Molins A , Galmés J. 2015. Surprisingly weak coordination between leaf structure and function among closely-related tomato species. *bioRxiv*, p. 031328.

Muir CD, Hangarter RP, Moyle LC , Davis PA. 2014a. Morphological and anatomical determinants of mesophyll conductance in wild relatives of tomato (*Solanum* sect. *Lycopersicon*, sect. *Lycopersicoides*; Solanaceae). *Plant, Cell & Environment*, **37**: 1415–1426.

Muir CD, Pease JB , Moyle LC. 2014b. Quantitative genetic analysis indicates natural selection on leaf phenotypes across wild tomato species (*Solanum* sect. *Lycopersicon*; Solanaceae). *Genetics*, **198**: 1629–1643.

Müller K , Wickham H. 2019. *tibble: Simple Data Frames.* R package version 2.1.1.

Nash JC. 2014. On best practice optimization methods in R. *Journal of Statistical Software*, **60**: 1–14.

Nash JC , Varadhan R. 2011. Unifying optimization algorithms to aid software system users: optimx for R. *Journal of Statistical Software*, **43**: 1–14.

bioRxiv preprint doi: https://doi.org/10.1101/601377; this version posted May 17, 2019. The copyright holder for this preprint (which was not certified by peer review) is the author/funder, who has granted bioRxiv a license to display the preprint in perpetuity. It is made available under aCC-BY 4.0 International license.

Nobel PS. 2009. *Physicochemical and Environmental Plant Physiology*. 4th edn. Academic Press, Oxford.

Olson ME , Arroyo-Santos A. 2015. How to study adaptation (and why to do it that way). *The Quarterly review of biology*, **90**: 167–191.

Parkhurst DF. 1978. The adaptive significance of stomatal occurrence on one or both surfaces of leaves. *The Journal of Ecology*, **66**: 367–383.

Parkhurst DF , Mott KA. 1990. Intercellular diffusion limits to CO_2 uptake in leaves studied in air and helox. *Plant Physiology*, **94**: 1024–1032.

Peat HJ , Fitter AH. 1994. A comparative study of the distribution and density of stomata in the British flora. *Biological Journal of the Linnean Society*, **52**: 377–393.

Pebesma E, Mailund T , Hiebert J. 2016. Measurement units in R. *The R Journal*, **8**: 486–494.

Poorter H, Niinemets Ü, Ntagkas N, Siebenkäs A, Mäenpää M, Matsubara S , Pons TL. 2019. A meta-analysis of plant responses to light intensity for 70 traits ranging from molecules to whole plant performance. *New Phytologist*.

Rogers A, Medlyn BE, Dukes JS, Bonan G, von Caemmerer S, Dietze MC, Kattge J, Leakey ADB, Mercado LM, Niinemets Ü *et al*. 2017. A roadmap for improving the representation of photosynthesis in earth system models. *New Phytologist*, **213**: 22–42.

Royer DL. 2001. Stomatal density and stomatal index as indicators of paleoatmospheric CO_2 concentration. *Review of Palaeobotany and Palynology*, **114**: 1–28.

Sack L , Buckley TN. 2016. The developmental basis of stomatal density and flux. *Plant Physiology*, **171**: 2358–2363.

Salisbury E. 1927. On the causes and ecological significance of stomatal frequency, with special reference to the woodland flora. *Philosophical Transactions of the Royal Society of London. Series B*, **216**: 1–65.

Šantrůček J, Schreiber L, Macková J, Vráblová M, Květoň J, Macek P , Neuwirthová J. 2019. Partitioning of mesophyll conductance for CO_2 into intercellular and cellular components using carbon isotope composition of cuticles from opposite leaf sides. *Photosynthesis Research*, pp. 1–19.

Sharkey TD, Bernacchi CJ, Farquhar GD , Singsaas EL. 2007. Fitting photosynthetic carbon dioxide response curves for C_3 leaves. *Plant, Cell & Environment*, **30**: 1035–1040.

Slot M , Winter K. 2017. In situ temperature relationships of biochemical and stomatal controls of photosynthesis in four lowland tropical tree species. *Plant, Cell & Environment*, **40**: 3055–3068.

Taylor SE. 1975. *Optimal leaf form*, Springer-Verlag, New York, pp. 73–86.

Vaughan D , Dancho M. 2018. *furrr: Apply Mapping Functions in Parallel using Futures*. R package version 0.1.0.

Vömdel H. 2016. Saturation vapor pressure formulations.

bioRxiv preprint doi: https://doi.org/10.1101/601377; this version posted May 17, 2019. The copyright holder for this preprint (which was not certified by peer review) is the author/funder, who has granted bioRxiv a license to display the preprint in perpetuity. It is made available under aCC-BY 4.0 International license.

Wickham H. 2011. The split-apply-combine strategy for data analysis. *Journal of Statistical Software*, **40**: 1–29.

Wickham H. 2016. *ggplot2: Elegant Graphics for Data Analysis*. Springer-Verlag New York.

Wickham H. 2018. *stringr: Simple, Consistent Wrappers for Common String Operations*. R package version 1.3.1.

Wickham H, François R, Henry L , Müller K. 2018. *dplyr: A Grammar of Data Manipulation*. R package version 0.7.8.

Wickham H , Henry L. 2018. *tidyr: Easily Tidy Data with 'spread()' and 'gather()' Functions*. R package version 0.8.2.

Wolfe JA. 1971. Tertiary climatic fluctuations and methods of analysis of Tertiary floras. *Palaeogeography, Palaeoclimatology, Palaeoecology*, **9**: 27–57.

Woodward FI. 1987. Stomatal numbers are sensitive to increases in CO_2 from pre-industrial levels. *Nature*, **327**: 617–618.

bioRxiv preprint doi: https://doi.org/10.1101/601377; this version posted May 17, 2019. The copyright holder for this preprint (which was not certified by peer review) is the author/funder, who has granted bioRxiv a license to display the preprint in perpetuity. It is made available under aCC-BY 4.0 International license.

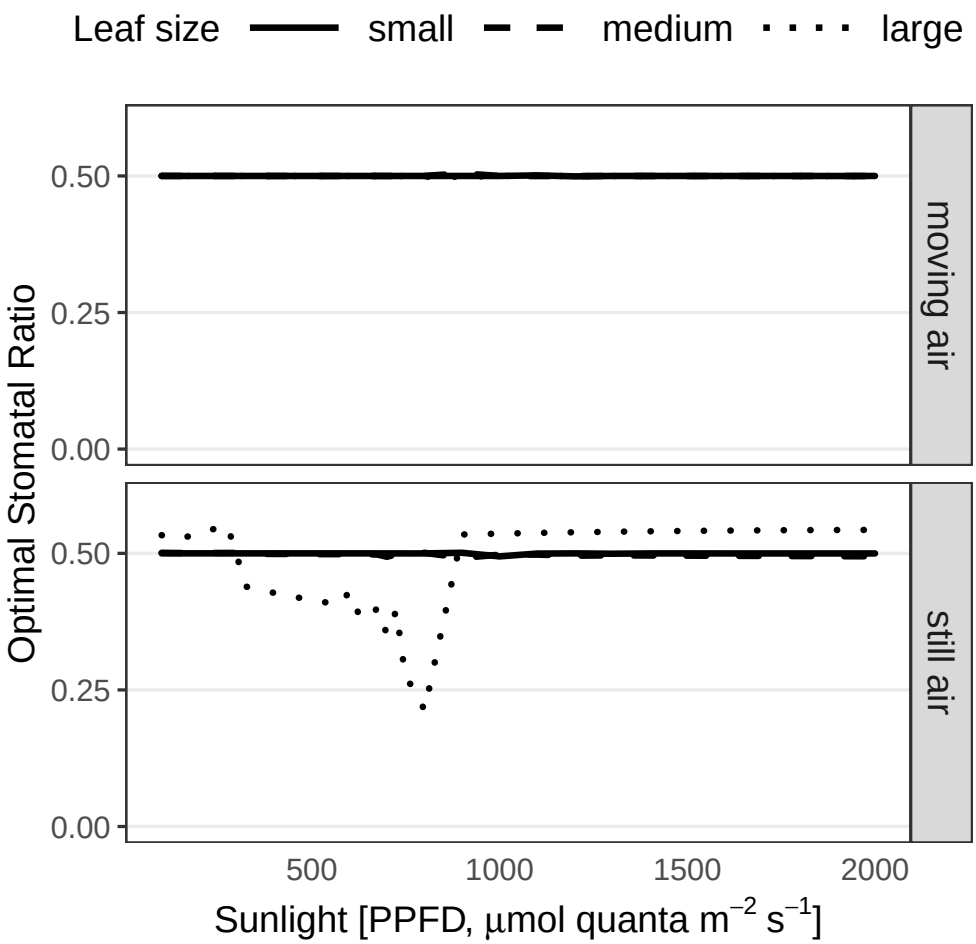

Figure 3: Model 1 shows that amphistomy is almost always optimal when there is no extrinsic cost. The optimal stomatal ratio SR_{opt} (*y*-axis) along a PPFD gradient (*x*-axis) for small ($d = 0.004$ m, solid lines), medium ($d = 0.04$ m, dashed lines), and large ($d = 0.4$ m, dotted lines) leaves. In moving air ($u = 2$ m s^{-1}, upper facet), amphistomy is always favored; all lines overlap at $SR_{\mathrm{opt}} \approx 0.5$. In still air ($u = 0.2$ m s^{-1}, lower facet), $SR_{\mathrm{opt}} < 0.5$ only occurs for large leaves in partial shade. Only results for T_{leaf} = 25 °C and $J_{\mathrm{max},25} = 75$ shown, but results are qualitatively similar for other variable combinations (Fig. S3). See Table S2 for other parameter values.

bioRxiv preprint doi: https://doi.org/10.1101/601377; this version posted May 17, 2019. The copyright holder for this preprint (which was not certified by peer review) is the author/funder, who has granted bioRxiv a license to display the preprint in perpetuity. It is made available under aCC-BY 4.0 International license.

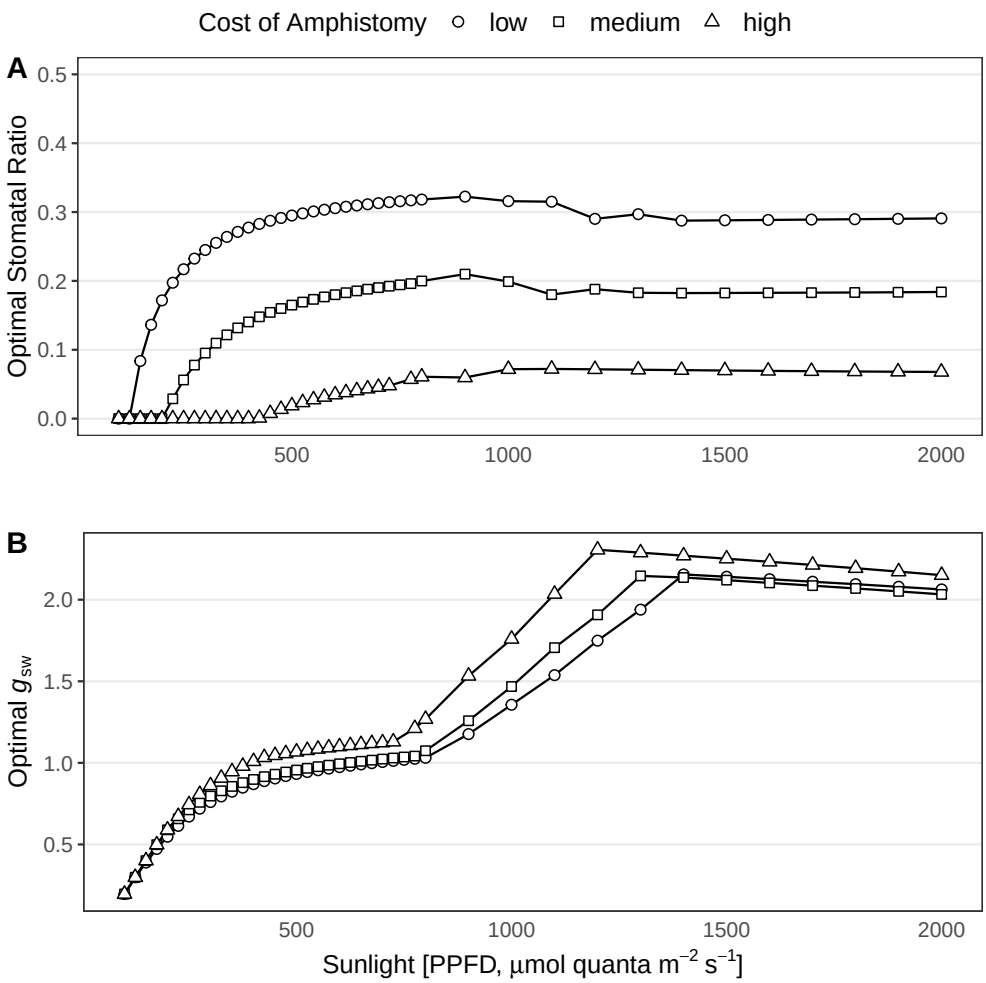

Figure 4: An extrinsic cost of amphistomy generates covariation between sunlight, stomatal ratio, and stomatal conductance. **A**) Model 2 predicts that optimal stomatal ratio (*y*-axis) increases with sunlight (*x*-axis). The optimal value depends on the cost of amphistomy (λ_{SR}^{-1}): high costs (triangles) favor hypostomy ($SR_{\mathrm{opt}} \approx 0$) over a broad range of light levels; low costs (circles) favor an intermediate value ($SR_{\mathrm{opt}} \approx 0.3$) at most light levels. **B**) Optimal stomatal conductance (g_{sw} [$\mu\mathrm{mol\ H_2O\ m^{-2}\ s^{-1}\ Pa^{-1}}$], *y*-axis) increases with sunlight, although the pattern is complex. The cost of amphistomy had relatively little effect on the shape of the relationship between sunlight and g_{sw}, because all three curves follow similar trajectories. See Table S3 for other parameter values.

bioRxiv preprint doi: https://doi.org/10.1101/601377; this version posted May 17, 2019. The copyright holder for this preprint (which was not certified by peer review) is the author/funder, who has granted bioRxiv a license to display the preprint in perpetuity. It is made available under aCC-BY 4.0 International license.

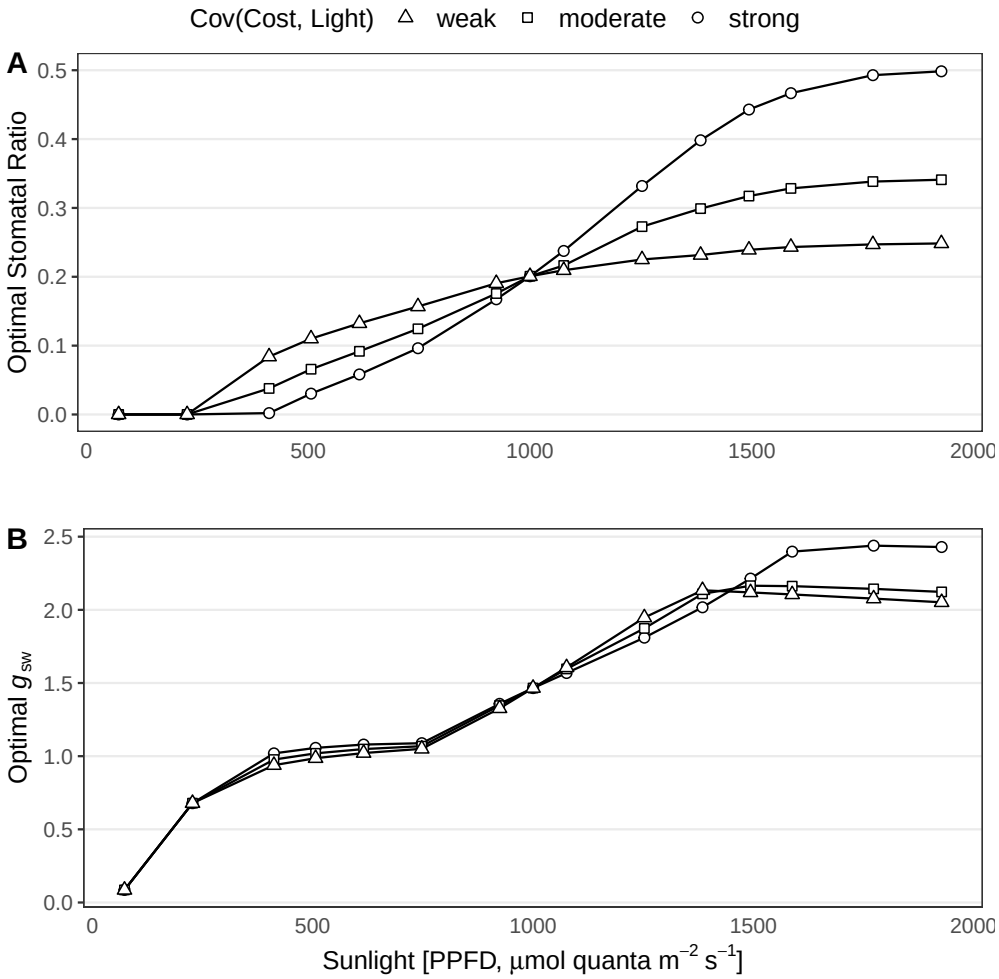

Figure 5: Strong covariance between an extrinsic cost of amphistomy (λ_{SR}^{-1}) and sunlight ["Cov(Cost, Light)"] generates threshold-like clines between sunlight, stomatal ratio, and stomatal conductance. **A**) Model 3 predicts that optimal stomatal ratio (*y*-axis) increases with sunlight (*x*-axis). When the covariance between costs and light is strong (circles), hypostomy is favored at low light, amphistomy is favored at high light, and there is a nonlinear transition between the two ends. Conversely, when the covariance is low (triangles), intermediate values of SR_{opt} are favored at high light, similar to Model 2. **B**) Optimal stomatal conductance (g_{sw} [$\mu\mathrm{mol\ H_2O\ m^{-2}\ s^{-1}\ Pa^{-1}}$], *y*-axis) increases with sunlight, although the pattern is complex. The covariance between cost and light had relatively little effect on g_{sw}, because all three curves follow similar trajectories. See Table S4 for other parameter values.

bioRxiv preprint doi: https://doi.org/10.1101/601377; this version posted May 17, 2019. The copyright holder for this preprint (which was not certified by peer review) is the author/funder, who has granted bioRxiv a license to display the preprint in perpetuity. It is made available under aCC-BY 4.0 International license.

Supporting Information

Photosynthetic temperature responses

I calcualted g_{mc}, Γ^*, J_{max}, K_{C}, K_{O}, R_{d}, V_{cmax}, and V_{tpu} at T_{leaf} (Table 2) based on an assumed value at 25 °C (Table 1) and temperature response paramters from (Bernacchi *et al.*, 2002, Table S1). Parameters with an exponentially increasing response to temperature were modeled as:

$$X_{T\mathrm{leaf}} = X_{25} e^{\frac{E_a}{\bar{R}T_{\mathrm{ref}}} \frac{T_{\mathrm{leaf}}-25}{T_{\mathrm{leaf}}-273.15}}$$

and those with a humped-shaped response were modeled as:

$$X_{T\mathrm{leaf}} = X_{25} e^{\frac{E_a}{\bar{R}T_{\mathrm{ref}}} \frac{T_{\mathrm{leaf}}-25}{T_{\mathrm{leaf}}-273.15}} \frac{1 + e^{[D_s/\bar{R} - E_d/(\bar{R}T_{\mathrm{ref}})]}}{1 + e^{(D_s/\bar{R}) - [E_d/(\bar{R}(T_{\mathrm{leaf}}+273.15))]}}$$

E_a and E_d are the enthalpies of activation and deactivation, respectively, and D_s is the entropy. T_{ref} is a reference temperature (25 °C) in K; T_{leaf} is a reference temperature in °C.

Table S1: Temperature response parameters

Parameter	E_a J mol^{-1}	E_d J mol^{-1}	D_s J mol^{-1} K^{-1}
g_{mc}	68901.56	487.29	148788.56
Γ^*	24459.97	-	-
J_{max}	56095.18	388.04	121244.79
K_{C}	80989.78	-	-
K_{O}	23719.97	-	-
R_{d}	40446.75	-	-
V_{cmax}	52245.78	-	-
V_{tpu}	52245.78	-	-

bioRxiv preprint doi: https://doi.org/10.1101/601377; this version posted May 17, 2019. The copyright holder for this preprint (which was not certified by peer review) is the author/funder, who has granted bioRxiv a license to display the preprint in perpetuity. It is made available under aCC-BY 4.0 International license.

Parameter conversions in leafoptimizer

Because of their differing origins and uses, leaf energy budget and photosynthesis models sometimes employ different units for the same parameter. As standalone packages, **tealeaves** and **photosynthesis** honor these conventions, but **leafoptimizer** must convert between them. Here I document these conversions.

As noted in the Materials and Methods section, conductance values are converted from m s^{-1} (**tealeaves**) to μmol m^{-2} s^{-1} Pa^{-1} (**photosynthesis**) using the ideal gas law:

$$g\ [\mathrm{m\ s^{-1}}] = \frac{g\ [\mu\mathrm{mol\ m^{-2}\ s^{-1}\ Pa^{-1}}]}{\bar{R}T}$$

Conductance to water vapor and CO_2 are interconverted using the the `gc2gw()` and `gw2qc()` functions:

$$g_w = g_c \frac{D_w}{D_c}$$

$$g_c = g_w \frac{D_c}{D_w}$$

Incident shortwave radiation (S_{sw} [W m^{-2}], **tealeaves**) is interconverted with PPFD [μmol quanta m^{-2} s^{-1}] (**photosynthesis**) following Gutschick (2016) using the functions `sun2ppfd()` and `ppfd2sun()`. Shortwave radiation is (at first approximation) the sum of photosynthetically active radiation (PAR) and near-infrared radiation (NIR):

$$S_{\mathrm{sw}} = S_{\mathrm{PAR}} + S_{\mathrm{NIR}}$$

Most sources (e.g. Jones, 2014) assume that $S_{\mathrm{PAR}} = S_{\mathrm{NIR}}$ for sunlight, so $f_{\mathrm{PAR}} = 0.5$. To convert PAR to PPFD, divide by the energy per mol quanta. assuming $E_q = 220$ kJ mol^{-1} quanta for PAR:

$$\mathrm{PPFD} = S_{\mathrm{PAR}}/E_q = f_{\mathrm{PAR}} S_{\mathrm{sw}}/E_q$$

tealeaves uses stomatal ratio (SR), while **photosynthesis** uses a partitioning factor k_{sc}. These are automatically interconverted as:

$$k_{\mathrm{sc}} = SR/(1 - SR)$$

bioRxiv preprint doi: https://doi.org/10.1101/601377; this version posted May 17, 2019. The copyright holder for this preprint (which was not certified by peer review) is the author/funder, who has granted bioRxiv a license to display the preprint in perpetuity. It is made available under aCC-BY 4.0 International license.

SI Figures

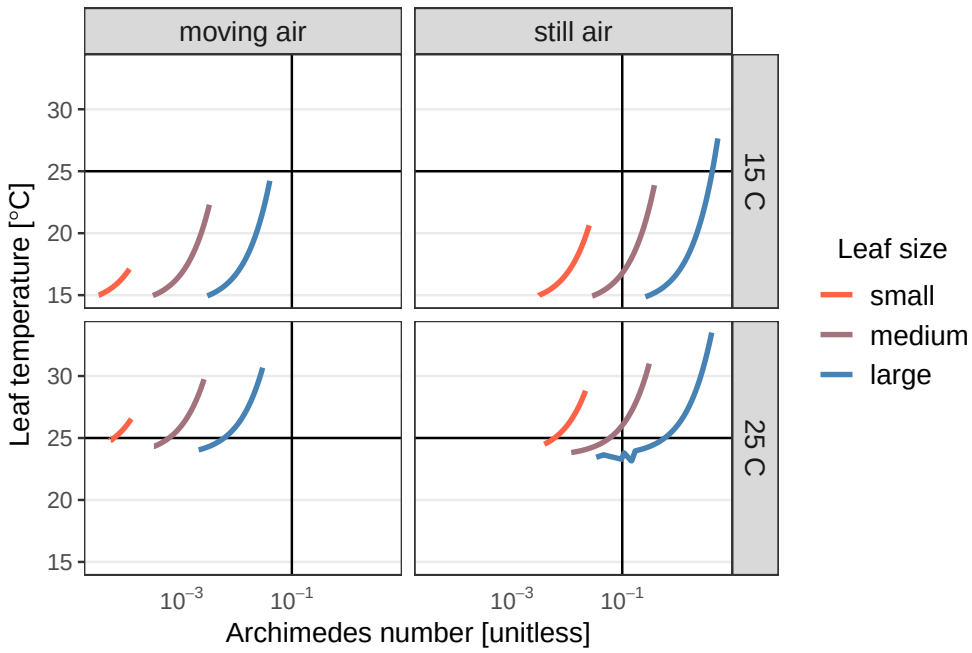

Figure S1: Environmental conditions that favor hypostomy are rare when there is no extrinsic cost to amphistomy. Each facet plots the Archimedes number (*x*-axis) against leaf temperature (*y*-axis) in moving air ($u = 2$ m s^{-1}, left column) and still air ($u = 2$ m s^{-1}, right column) at two air temperatures: $T_{\text{air}} = 15$ °C (top row) and $T_{\text{air}} = 25$ °C, (bottom row). Results from a third temperature ($T_{\text{air}} = 35$ °C) indicated bistability at intermediate Archimedes numbers and are not shown here, but results are archived online (see Materials and Methods). Hypostomy reduces transpiration, increasing leaf temperature, which can be beneficial when leaf temperatures are suboptimal for photosynthesis (approximately 25 °C, horizontal line in all facets). This only occurs at low air temperatures (top row). Furthermore, free convection must be significant (Archimedes number > 0.1, vertical line in all facets). This only occurs for medium and large leaves under high light, which generates a larger leaf-to-air temperature differential. See Table S2 for other parameter values.

bioRxiv preprint doi: https://doi.org/10.1101/601377; this version posted May 17, 2019. The copyright holder for this preprint (which was not certified by peer review) is the author/funder, who has granted bioRxiv a license to display the preprint in perpetuity. It is made available under aCC-BY 4.0 International license.

SI Figures

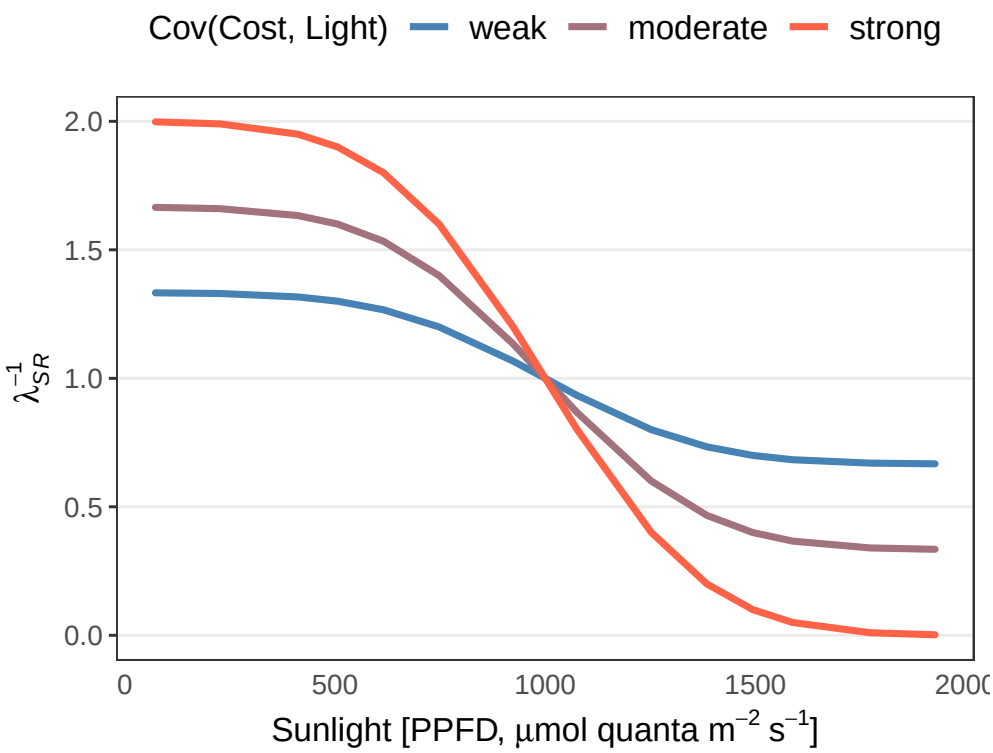

Figure S2: Weak, moderate, and strong examples of covariation ["Cov(Cost, Light)"] between light (PPFD, *x*-axis) and the cost of amphistomy (λ_{SR}^{-1} Pa, *y*-axis) used in Model 3. The inverse of λ_{SR} is plotted because as this value increases, the costs of amphistomy are greater. When the covariance is strong, λ_{SR}^{-1} has greater range over the same PPFD values compared to when the covariance is weak.

bioRxiv preprint doi: https://doi.org/10.1101/601377; this version posted May 17, 2019. The copyright holder for this preprint (which was not certified by peer review) is the author/funder, who has granted bioRxiv a license to display the preprint in perpetuity. It is made available under aCC-BY 4.0 International license.

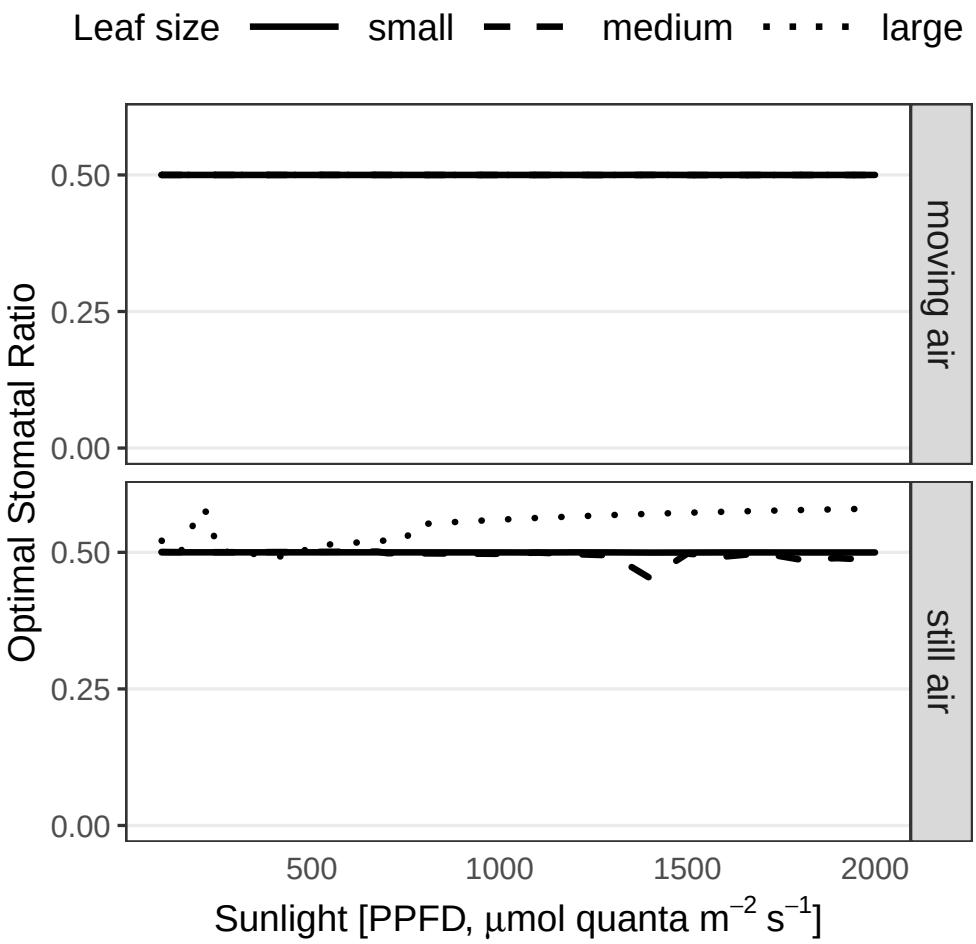

Figure S3: Model 1 shows that amphistomy is almost always optimal when there is no extrinsic cost, regardless of biochemical parameters. This figure is same as Fig. 3, except the biochemical parameters. The optimal stomatal ratio SR_{opt} (*y*-axis) along a PPFD gradient (*x*-axis) for small ($d = 0.004$ m, solid lines), medium ($d = 0.04$ m, dashed lines), and large ($d = 0.4$ m, dotted lines) leaves. In moving air ($u = 2$ m s^{-1}, upper facet), amphistomy is always favored; all lines overlap at $SR_{\mathrm{opt}} \approx 0.5$. Only results for T_{leaf} = 25 °C and $J_{\mathrm{max,25}} = 150$ shown. See Table S2 for other parameter values.

bioRxiv preprint doi: https://doi.org/10.1101/601377; this version posted May 17, 2019. The copyright holder for this preprint (which was not certified by peer review) is the author/funder, who has granted bioRxiv a license to display the preprint in perpetuity. It is made available under aCC-BY 4.0 International license.

SI Tables

bioRxiv preprint doi: https://doi.org/10.1101/601377; this version posted May 17, 2019. The copyright holder for this preprint (which was not certified by peer review) is the author/funder, who has granted bioRxiv a license to display the preprint in perpetuity. It is made available under aCC-BY 4.0 International license.

Table S2: Model 1 variable and parameter values. See Table 1 for symbol definitions and values of physical constants.

Symbol	Value(s)	Units
Variables:		
d	0.004, 0.04, 0.4	m
$J_{\mathrm{max},25}$	75, 150	μmol CO_2 m^{-2} s^{-1}
PPFD	100 – 2000	μmol quanta m^{-2} s^{-1}
u	0.2, 2	m s^{-1}
$V_{\mathrm{cmax},25}$	2/3 $J_{\mathrm{max},25}$	μmol CO_2 m^{-2} s^{-1}
Carbon costs:		
$\lambda_{\mathrm{w}}^{-1}$	0.001	mol CO_2 mol^{-1} H_2O
λ_{SR}^{-1}	0	Pa
Fixed leaf parameters:		
α_{s}	0.5	none
α_{l}	0.97	none
$g_{\mathrm{mc},25}$	3	μmol CO_2 m^{-2} s^{-1} Pa^{-1}
g_{uc}	0.1	μmol CO_2 m^{-2} s^{-1} Pa^{-1}
Γ^*_{25}	3.743	Pa
$K_{\mathrm{C},25}$	27.238	Pa
$K_{\mathrm{O},25}$	16.582	kPa
k_{mc}	1	none
k_{uc}	1	none
ϕ_J	0.331	none
$R_{\mathrm{d},25}$	2	μmol CO_2 m^{-2} s^{-1}
θ_J	0.825	none
$V_{\mathrm{tpu},25}$	200	μmol CO_2 m^{-2} s^{-1}
Fixed environmental parameters:		
C_{air}	41	Pa
E_q	220	kJ mol^{-1}
f_{PAR}	0.5	none
O	21.27565	kPa
P	101.3246	kPa
r	0.2	none
RH	0.5	none

bioRxiv preprint doi: https://doi.org/10.1101/601377; this version posted May 17, 2019. The copyright holder for this preprint (which was not certified by peer review) is the author/funder, who has granted bioRxiv a license to display the preprint in perpetuity. It is made available under aCC-BY 4.0 International license.

Table S3: Model 2 variable and parameter values. See Table 1 for symbol definitions and values of physical constants.

Symbol	Value(s)	Units
Variables:		
PPFD	100 – 2000	μmol quanta m^{-2} s^{-1}
Carbon costs:		
$\lambda_{\mathrm{w}}^{-1}$	0.001	mol CO_2 mol^{-1} H_2O
λ_{SR}^{-1}	0.5, 1, 2	Pa
Fixed leaf parameters:		
α_{s}	0.5	none
α_{l}	0.97	none
d	0.1	m
$J_{\mathrm{max,25}}$	112.5	μmol CO_2 m^{-2} s^{-1}
$g_{\mathrm{mc,25}}$	3	μmol CO_2 m^{-2} s^{-1} Pa^{-1}
g_{uc}	0.1	μmol CO_2 m^{-2} s^{-1} Pa^{-1}
Γ^*_{25}	3.743	Pa
$K_{\mathrm{C,25}}$	27.238	Pa
$K_{\mathrm{O,25}}$	16.582	kPa
k_{mc}	1	none
k_{uc}	1	none
ϕ_J	0.331	none
$R_{\mathrm{d,25}}$	2	μmol CO_2 m^{-2} s^{-1}
θ_J	0.825	none
u	2	m s^{-1}
$V_{\mathrm{cmax,25}}$	2/3 $J_{\mathrm{max,25}}$	μmol CO_2 m^{-2} s^{-1}
$V_{\mathrm{tpu,25}}$	200	μmol CO_2 m^{-2} s^{-1}
Fixed environmental parameters:		
C_{air}	41	Pa
E_q	220	kJ mol^{-1}
f_{PAR}	0.5	none
O	21.27565	kPa
P	101.3246	kPa
r	0.2	none
RH	0.5	none

bioRxiv preprint doi: https://doi.org/10.1101/601377; this version posted May 17, 2019. The copyright holder for this preprint (which was not certified by peer review) is the author/funder, who has granted bioRxiv a license to display the preprint in perpetuity. It is made available under aCC-BY 4.0 International license.

Table S4: Model 3 variable and parameter values. See Table 1 for symbol definitions and values of physical constants.

Symbol	Value(s)	Units
Variables:		
PPFD	73 – 1927	μmol quanta m^{-2} s^{-1}
Carbon costs:		
$\lambda_{\mathrm{w}}^{-1}$	0.001	mol CO_2 mol^{-1} H_2O
λ_{SR}^{-1}	0.002 – 1.998	Pa
Fixed leaf parameters:		
α_{s}	0.5	none
α_{l}	0.97	none
d	0.1	m
$J_{\mathrm{max,25}}$	112.5	μmol CO_2 m^{-2} s^{-1}
$g_{\mathrm{mc,25}}$	3	μmol CO_2 m^{-2} s^{-1} Pa^{-1}
g_{uc}	0.1	μmol CO_2 m^{-2} s^{-1} Pa^{-1}
Γ^*_{25}	3.743	Pa
$K_{\mathrm{C,25}}$	27.238	Pa
$K_{\mathrm{O,25}}$	16.582	kPa
k_{mc}	1	none
k_{uc}	1	none
ϕ_J	0.331	none
$R_{\mathrm{d,25}}$	2	μmol CO_2 m^{-2} s^{-1}
θ_J	0.825	none
u	2	m s^{-1}
$V_{\mathrm{cmax,25}}$	2/3 $J_{\mathrm{max,25}}$	μmol CO_2 m^{-2} s^{-1}
$V_{\mathrm{tpu,25}}$	200	μmol CO_2 m^{-2} s^{-1}
Fixed environmental parameters:		
C_{air}	41	Pa
E_q	220	kJ mol^{-1}
f_{PAR}	0.5	none
O	21.27565	kPa
P	101.3246	kPa
r	0.2	none
RH	0.5	none